ARTICLE

BIOTECHNOLOGY and BIOENGINEERING

Genomic and Proteomic Exploration of CHO and Hybridoma Cells Under Sodium Butyrate Treatment

Joon Chong Yee,[1] Marcela de Leon Gatti,[1] Robin J. Philp,[2] Miranda Yap,[2] Wei-Shou Hu[1]

[1]Department of Chemical Engineering and Materials Science, University of Minnesota, 421 Washington Avenue SE, Minneapolis, MN 55455-0132; telephone: 612-626-7630; fax: 612-626-7246; e-mail: acre@cems.umn.edu

[2]Bioprocessing Technology Institute, A-Star, Centros, Singapore

Received 7 March 2007; revision received 2 July 2007; accepted 14 September 2007

Published online 10 October 2007 in Wiley InterScience (www.interscience.wiley.com). DOI 10.1002/bit.21665

ABSTRACT: Sodium butyrate has been known to increase the specific productivity of recombinant proteins in mammalian cells. In quest of physiological mechanisms leading to the increased productivity, DNA microarray and two dimensional gel electrophoresis (2DE) were used to assess the response of Chinese hamster ovary (CHO) and a mouse hybridoma cell (MAK) to butyrate treatment at the transcriptome and proteome level. The expression of the orthologous genes represented on both CHO cDNA and mouse Affymetrix microarray, as well as genes in the same ontological class were compared. Only a relatively small number of orthologs changed their expression consistently between the two cell lines, however, at a functional class level many genes involved in cell cycle and apoptosis were affected in both cell lines. Furthermore, a large number of genes involved in protein processing, secretion and redox activity were upregulated in both CHO and MAK cells. More genes showed a consistent trend of change at both transcript and protein levels than those which showed opposite trend in MAK cells. Overall the results suggested that the changes arising in the protein processing machinery may be responsible for the increased productivity upon butyrate treatment in both CHO and MAK cells.

Biotechnol. Bioeng. 2008;99: 1186–1204.

KEYWORDS: transcriptome; proteome; microarray; cell culture; protein secretion; recombinant protein

Introduction

Recombinant antibodies are currently the most important biologics produced in mammalian cell culture. Given their importance as a therapeutic agent, the demand for recombinant antibodies has increased rapidly in the past decade. To meet this high-volume demand, several strategies have been employed to increase antibody titer in bioproduction. Some of these methods include increasing final cell concentration in the reactor by controlled feeding processes (Zhou et al., 1995), and improved media composition (Farges-Haddani et al., 2006). Emphasis has also been placed on cell line development (Wurm, 2004) and cell engineering (Mazur et al., 1998) to construct a cell line with enhanced specific protein productivity. Others have explored varying culture conditions, such as low temperature (Barnabe and Butler, 1994; Fogolin et al., 2004; Yoon et al., 2003), high osmolarity (Shen and Sharfstein, 2006) and sodium butyrate treatment (Cherlet and Marc, 2000; Chun et al., 2003; de Leon Gatti et al., 2007) to elicit a higher productivity from mammalian cells. Sodium butyrate has been shown to increase productivity in CHO (de Leon Gatti et al., 2007; Kim and Lee, 2000; Mimura et al., 2001) and hybridoma (Cherlet and Marc, 2000; Oh et al., 1993) cell lines. Increased titer in other recombinant proteins such as erythropoietin (Wang et al., 2002), tissue plasminogen activator (Hendrick et al., 2001), follicle stimulating hormone (Chotigeat et al., 1994) and factor VIII (Chun et al., 2003) have also been reported in CHO cells undergoing sodium butyrate treatment. However, the positive effect on titer can be offset by its detrimental effect on cell growth, viability and quality of the recombinant protein.

Mechanistically, butyrate acts as a histone deacetylase inhibitor which facilitates the "opening" of chromatin to the access of transcription factors (Riggs et al., 1977). Additionally, butyrate has been reported to cause a wide range of effects on gene expression in cultured mammalian cells. Improvements in transient expression and enhanced stable transfection efficiency were reported in HeLa and CV1 cells when treated with butyrate immediately following transfection (Gorman et al., 1983). Aside from its influence in the uptake of foreign DNA, butyrate also enhances the expression of heterologous genes under the control of major

Correspondence to: W.-S. Hu

Contract grant sponsor: NIH Biotechnology

Contract grant number: GM08347

mammalian promoters including cytomegalovirus (CMV) and simian virus 40 (Palermo et al., 1991). Whilst butyrate is known to increase the expression of heterologous gene, the global phenotypic changes undergone by cells to secrete higher quantities of recombinant protein have yet to be elucidated.

Recently DNA microarrays and proteomic analysis have been used to investigate gene expression of mammalian cells under different culture conditions such as high osmolarity (Shen and Sharfstein, 2006), low temperature (Baik et al., 2006) and metabolic shift (Korke et al., 2004). Quantitative protein 2-D gel (Dinnis et al., 2006) and stable isotope peptide labeling combined with DNA microarray (Seth et al., 2006) have been utilized to compare the NS0 clones exhibiting a range of antibody productivity.

Using those global gene expression profiling tools to survey cells with varying levels of productivity can reveal the expression phenotype which leads to hyperproductivity. However, such effort will also require the examination of a large number of clones. By probing gene expression profiles of cells under conditions which increase productivity one may gain insight to the critical pathways that contribute to this phenotype. In this study we chose to examine the effect of butyrate on gene expression in two different cell lines to further shed light on the relationship between gene expression and the complex traits of hyperproductivity.

Our laboratory has previously probed the expression of CHO cells following butyrate treatment by utilizing mouse cDNA array and a prototype CHO microarray (de Leon Gatti et al., 2007). Results from cross-species CHO:mouse and CHO:CHO array hybridizations were compared. CHO:mouse cross-species hybridizations were not very revealing because differential gene expression often could not be called with a high degree of statistical confidence.

We have since developed DNA microarrays containing a larger number of gene probes. In this study, we sought to identify gene expression changes caused solely by butyrate, therefore, RNA from cells in the absence and presence of butyrate were compared directly after 27 h treatment, where the largest amount of gene perturbation were previously found (de Leon Gatti et al., 2007). Transcriptome results were further complemented by two-dimensional protein gel electrophoresis to investigate the impact of butyrate at the protein level. Comparison of the transcript and protein changes in these two important cell lines is the first step to ascribing genes related to increased protein productivity.

Materials and Methods

Cell Culture Conditions

Mouse-mouse hybridoma and recombinant CHO cells used have been reported previously (de Leon Gatti et al., 2007). The hybridoma cells were grown in a defined medium consisting of a 1:1 mixture of Dulbecco's modified Eagle's medium (DMEM) and Ham's F12 medium supplemented with 63.7 nM transferrin, 23.7 μM 2-mercaptoethanol, 1.7 mM ethanolamine, 0.11 mM L-ascorbic acid, 28.9 nM sodium selenite and 6.2 μM putrescine. The recombinant CHO cells were grown in the same media, and were additionally supplemented with 0.15 mM methotrexate (MTX) and 0.01% (v/v) intralipid emulsion (Sigma–Aldrich, St. Louis, MO). Sodium butyrate (Sigma–Aldrich) was added to a final concentration of 1 mM in the cultures after 24 h of inoculation. The inoculum was at 2.5×10^5 cells/mL. Cells were grown in cell culture T-flasks in stationary mode in a 37°C, 5% CO_2 environment. Cell concentration and viability were evaluated with a hemocytometer and trypan blue staining.

Microarrays

DNA Arrays

The construction of the CHO cDNA libraries and microarray has been previously described (Wlaschin et al., 2005). The CHO cDNA microarray contained 14,112 EST sequences derived from two cDNA libraries and the Affymetrix MOE430A array contains 22,690 probes representing 13,147 well characterized mouse genes. Orthologous genes in the MOE430A and CHO cDNA array were identified by performing Basic Local Alignment Search Tool (BLAST) on probe sequences from MOE430A against those on the CHO microarray (Altschul et al., 1990). Any pair of sequences with a BLAST score above 200, and an e-value criterion below 10^{-25} was identified as orthologs.

Sample Preparation

Cell samples were taken from duplicate cultures at 27 h after butyrate addition. Cells were pelleted by centrifugation at 700 rpm for 5 min and stored in liquid nitrogen until RNA extraction. Total RNA was extracted with the RNeasy kit (Qiagen, Valencia, CA) followed by DNAse treatment. Purity and integrity of RNA was verified by running 2 μg of RNA in a 1.4% agarose gel in 10 mM sodium phosphate buffer, pH 6.8 at 100 V (Pelle and Murphy, 1993). The concentration of RNA was estimated by measuring the absorbance at 260 nm.

CHO cDNA Microarray

Hybridization and Scanning

The sample preparation of total RNA for hybridization on cDNA array has been described previously. (Wlaschin et al., 2005). Image analysis and visualization were performed with GenePix™ Pro 4.1 (Molecular Devices Corporation, Union

City, CA). After subtracting from background, signal intensities were normalized using the LOWESS (Locally Weighted Regression and Smoothing Scatter Plots) method available in GeneSpring® (Silicon Genetics, Redwood City, CA) to compensate for different dye labeling effects. Four replicates which include two pairs of dye swap were conducted for each hybridization on the CHO array.

Data Analysis

The mean and standard deviation of the log_2-transformed ratio for each spot were calculated from the replicated microarray experiments. Outliers that have log_2-transformed ratio greater than 1.5 times the standard deviation were discarded. The average of the log-ratios for each spot was calculated. A paired difference *t*-test was performed for replicate spots using the average log_2-transformed ratio, corresponding standard deviation, and number of replicates. Among these sequences, only those whose average log_2-transformed ratio was equal to or greater than 0.485 (i.e., arithmetic fold change $\geq$1.4) and with a *P*-value lower than 0.05 were considered as candidate differentially expressed sequences. For the genes represented by more than one sequence on the microarray, the probe sequence that yields a *P*-value less than 0.05 were considered for the analysis, and at least 50% of these sequences have to pass the log_2 criterion of equal to or greater than 0.485 criterion for the gene to be considered as differentially expressed.

Mouse Affymetrix MOE430A GeneChip

Hybridization and Scanning

Sample preparation of RNA and hybridization to MOE430A GeneChip were performed as described in the Affymetrix Technical Manual and described in previous publication (Seth et al., 2005). The gene chips were scanned using the GeneChip® Scanner 3000 (Affymetrix, Santa Clara, CA) at high resolution setting. Two arrays each for the control culture and sodium butyrate-treated culture were hybridized. The final intensity for the data obtained from the four chips was analyzed with the GeneData Expressionist software 4.0 and the data was de-convoluted by the Li-Wong method.

Data Analysis

Logarithmic mean normalization was applied to all the probe intensity to an average of 1,000. The analysis generates a ''detection *P*-value,'' which indicates the target specific hybridization intensity. A detection *P*-value $<$0.04 indicates a transcript is reliably detected and this criterion is applied throughout the microarray data analysis. Genes were further analyzed for differential expression by performing a *t*-test on the two chips for each sample (butyrate treated and control). Genes with higher than 95% confidence in the *t*-test (*P*-value $<$0.05) and have a 1.4-fold change were identified as being differentially expressed.

Proteomics

Sample Preparation and 2D Gel Electrophoresis

Cells harvested after 27 h of sodium butyrate treatment were centrifuged and washed twice with PBS. Two hundred microliters of lysis solution (7 M Urea, 2 M Thiourea, 4% CHAPS, 50 mM Tris pH 8.0, protease inhibitor cocktail (Sigma–Aldrich), DNAse, RNAse) was added to the cell pellet followed by brief vortexing. The cell lysate were assayed for protein concentration using Coomassie blue dye binding (Pierce, Rockford, IL) and then stored at -80°C until subsequent analysis.

All samples for separation by two-dimensional gel electrophoresis (2-DE) were diluted into a re-hydration solution (7 M urea, 2 M thiourea, 4% CHAPS, 20 mM dithiothreitol, 0.2% IPG buffer (GE-Healthcare, Uppsala, Sweden)) and a trace of bromophenol blue. Each gel loading consisted of 120 μg of total protein with four replicate gel runs for each sample. First dimensional separation was carried out using 18 cm IPG strips 3-10 NL (GE-Healthcare) with the following conditions: 200 V (100 Vh), 500 V (250 Vh), 1,000 V (500 Vh), 8,000 V (2,250 Vh) and 8,000 V (24,000 Vh). Following the iso-electric focusing, the IPG strips were equilibrated in 6 M urea, 30% glycerol, 50 mM Tris, pH 6.8, 2% SDS and 1% w/v DTT for 15 min on a shaking platform. The solution was discarded, replaced with 6 M urea, 30% glycerol, 50 mM Tris pH 8.8, 2% SDS and 2.5% w/v iodoacetamide and incubated for another 15 min. The IPG strips were drained and then embedded in molten agarose on top of 10% uniform polyacrylamide gels measuring 18 cm $\times$ 18 cm. The gel cassettes (Bio-Rad Protean II) were assembled and running buffer added to the upper and lower chambers (25 mM Tris-base, 192 mM glycine, 0.1% SDS). Separation was carried out at 30 mA per gel until the dye front had reached the end of the gel. Following electrophoresis gels were removed from the cassettes and fixed in 50% methanol/10% acetic acid and stained using Sypro Orange (Invitrogen, Carlsbad, CA) according to the manufacturer's instructions.

Gels were scanned using a Typhoon 8600 scanner (GE-Healthcare) and the images stored digitally. The images were processed for analysis using PDQuest 6.0 software (Bio-Rad, Hercules, CA) where spot detection with Gaussian fitting, background subtraction and spot matching were performed. The images were manually re-examined and corrected for undetected, falsely-detected and unmatched spots. Normalization based on total density of each gel image was also performed to eliminate any bias arising from variations other than biological expression. Differentially expressed spots were determined based on significance criteria of at least a 1.5-fold change and a *P*-value $<$0.05 using student's *t*-test.

All protein spots that were shown to be differentially expressed by 1.5-fold or greater were excised for identification. Excised protein spots were subjected to in-gel proteolysis with trypsin following reduction and s-alkylation of cysteine residues with iodoacetamide. The peptide pools obtained were concentrated using a Speed-Vac (Savant, Holbrook, NY) and re-solubilized in 1% formic acid/2% methanol prior to analysis by mass spectrometry.

Mass Spectrometry and Identification of Gel Separated Proteins

Identification of proteins was made by subjecting the peptide pool from each in-gel digested gel spot to nano-liquid chromatography-tandem mass spectrometry (nanoLC-MS/MS). Briefly, each sample was injected onto a C-18 reversed-phase micro-pre-column in 0.1% formic acid (Sigma–Aldrich) at 25 μL/min. Following a 5 min wash with the same solvent the column was switched in line with a gradient elution onto a 75 μm × 10 cm C18 reversed-phase column (packed in-house). Elution was performed using a linear gradient of 0.1% formic acid in HPLC grade water to 0.1% formic acid in 60% acetonitrile over 40 min at 130 nL/min. Eluting peptides were ionized by the application of 2200 V applied distally to the column and sprayed directly into a QSTAR-XL (ABI/MDS-SCIEX, Foster City, CA) quadrupole time-of-flight tandem mass spectrometer (Qqtof) operating in information dependant analysis mode (IDA). Each multiply-charged (2^+ and 3^+) peptide mass ion with a threshold greater than eight counts per second within a mass range of 300 and 2,000 amu was selected for fragmentation and subsequent MS/MS analysis using nitrogen as the collision gas and a rolling collision energy under the control of the Analyst QS operating software version 1.1. All MS/MS data files were searched against either the *Mus*, *Rodentia*, or *Mammalia* subset of the UniProt protein database (EBI, Cambridge, UK, download date 20060404 containing 2,952,845 sequences) using the MS/MS ion search component of the MASCOT search engine (MatrixScience, London, UK). Allowance for the oxidation of methionine residues and alkylation (carbamidomethylation) of cysteine residues was made as well as a peptide mass tolerance of 150 ppm and a MS/MS tolerance of 0.5 Da. For a protein to be confidently identified at least two unique peptides had to match to the protein with a score equal or greater than that calculated by the software to give identification with 95% probability.

Results

Overall Transcriptome Changes on CHO and Hybridoma

We have shown previously that sodium butyrate treatment increased antibody production by at least twofold in both a recombinant CHO cell line and a mouse hybridoma MAK cell line (de Leon Gatti et al., 2007). To probe transcriptome changes in response to butyrate treatment exponentially growing CHO and MAK cells were treated with 1 mM sodium butyrate. After 27 h of treatment, before viability was significantly decreased, cells were harvested. Their mRNA transcript levels were probed using CHO cDNA and Affymetrix MOE340A microarray respectively. The mouse MOE430A microarray used had 13,971 unique gene probes while the CHO array contained 6,822 unique gene probes. Genes with at least 1.4-fold changes in transcript levels between sodium butyrate treated and control cases as well as a P-value <0.05 were identified. Based on this criterion, 578 genes were increased (4.1% of gene probes) and 643 decreased in MAK (4.6% of gene probes). Amongst these genes, 174 had at least a twofold change. Applying a similar statistical criterion to the gene expression of CHO cells, 482 genes were differentially expressed in a positive trend (7% of gene probes) while 260 genes had reduced expression (3.8% of gene probes) upon sodium butyrate treatment. However, only 10 genes were differentially expressed greater than twofold.

Ontological classes for the genes represented on both arrays were obtained from GenMapp (www.genmapp.org) using the annotated mouse unigene ID. The differentially expressed and well annotated genes (919 and 604 for MAK and CHO, respectively) were classified according to biological process ontology. The ontological classes for which at least 10% of the gene probes on the array in that class had differentially expressed are listed in Figure 1.

For MAK cells, approximately 20–30% of glycolysis and cholesterol synthesis genes probed were differentially expressed. For CHO, the extent of changes in these metabolic pathways were less significant, however the number of gene probes on the array was also smaller. Among those ontological classes listed in Figure 1 apoptosis, cell cycle, protein folding and protein transport have larger number of genes differentially expressed for both MAK and CHO.

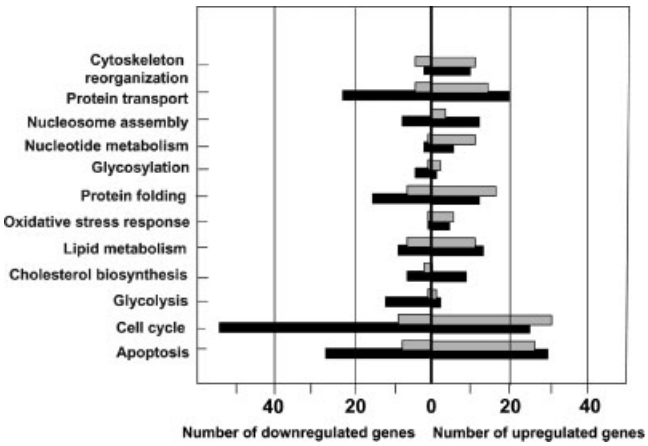

Figure 1. Distribution of differentially expressed genes in gene ontological classes that were affected by sodium butyrate for MAK (■) and CHO (▒).

Comparative Expression Profile of CHO and MAK Gene Orthologs

To compare the response of CHO and MAK, the *log-2* transformed ratio of transcript levels at the butyrate treated and control conditions for 1205 orthologous gene probes present on CHO and MOE430A microarray were plotted (Fig. 2). Panel A and B shows only data points with >1.4-fold change and *P*-value ≤0.05 on the mouse and CHO array respectively. Transcripts with a *P*-value ≤0.05 in both MAK and CHO are shown in filled circles.

Twenty three genes responded similarly to butyrate treatment in CHO and MAK (data points in regions S and S′ in Fig. 2A and B). Upon closer examination, only 11 of the 23 orthologs (dark circles in regions S and S′) yield a *P*-value ≤0.05 in both arrays. Among these 11 orthologs, eight transcripts were increased and three decreased upon sodium butyrate treatment. The transcripts which increased include three genes involved in redox balance (microsomal glutathione S-transferase 3, glutathione S-transferase alpha 1 and selenoprotein P plasma 1) and two responsive towards protein overload in the endoplasmic reticulum (eukaryotic initation factor 2 alpha kinase 3 and glucose regulated protein 78 kDa) (shown in Table IV). Other transcripts that showed positive fold changes are histone 3B, cathepsin L (Data not shown) and cyclin D (Table II). Transcripts which decreased in both CHO and MAK include lactate dehydrogenase 1A (Fig. 3), programmed cell death 4 (Table III) and chromosome segregation 1-like protein (Table II).

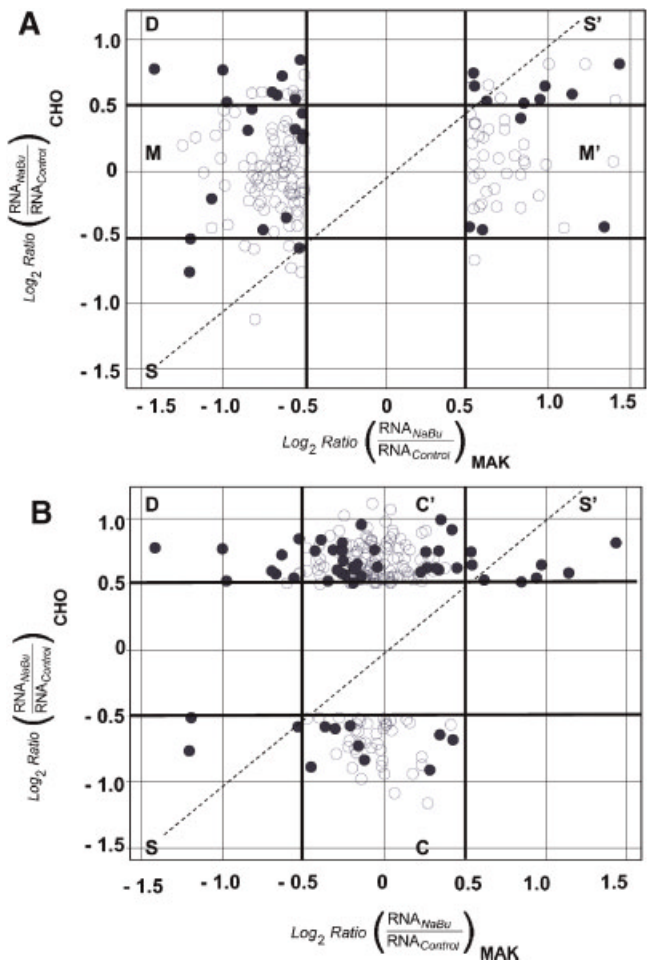

Figure 2. Comparison of $\log_2$ intensity ratios of RNA from sodium butyrate treated and control culture for 1205 gene orthologs in both CHO and MOE430A mouse array. Dark circles represent log intensity ratios with *P*-value ≤0.05 in both CHO and MOE430A array. Open circles are those with a *P*-value ≤0.05 only in the CHO array (**A**) or only in the MOE430A array (**B**). [Color figure can be seen in the online version of this article, available at www.interscience.wiley.com.]

Regions M and M′ in Figure 2 highlights 127 genes which were differentially expressed in MAK but remained unchanged in CHO. Twelve of these genes had a greater than twofold change in MAK. Likewise, 167 genes were differentially expressed in CHO but with no evidence of transcript changes occurring in MAK (Fig. 2 B, highlighted in regions C and C′). Five genes which were differentially expressed in opposite trends between CHO and MAK lie inside region D. They consist of a protein folding chaperone: Von-Hippel Lindau binding protein 1 (Table IV), two cell cycle/chromosome modification gene: Telomere repeat binding factor 1, chromosome-condensation related SMC associated protein 1 (Table II) and two RNA processing genes (Data not shown).

Thus the two cell lines do exhibit substantial difference in their response to butyrate treatment. A listing of these genes along with their expression level fold change are listed according to their functional classes and provided in Tables I–IV. For easy comparison between MAK and CHO the differentially expressed genes are highlighted in bold. The majority of CHO and mouse orthologs are not differentially expressed in either cell line. More differentially expressed genes are specific to one cell line than common to both. To gain physiological insight on the other transcript changes, the major ontological classes which are affected by sodium butyrate are discussed in the following sections.

Glycolysis and TCA Cycle Pathway

The glycolysis and TCA cycle genes probed for MAK cells are shown in Figure 3 with the corresponding fold change values. Isozymes for the same enzyme are shown in multiple boxes that share the same border. Subunits of an enzyme or enzyme complex (e.g., pyruvate dehydrogenase complex) are enclosed in a thick border. Among the 21 glycolysis enzymes represented on the mouse array, 13 were differentially expressed in MAK. With the exception of hexokinase 2 and phosphoglycerate mutase 2, all the other 11 genes showed reduced transcript expression.

All 18 TCA cycle genes are represented on the MOE430A array. Two isofoms of succinyl CoA synthase showed decreased expression with a *P*-value <0.05. Three subunits of the pyruvate dehydrogenase complex were also decreased >1.5-fold, this enzyme complex is responsible for converting pyruvate into acetyl-CoA. Pyruvate can also be

converted to oxaloacetate through the enzyme pyruvate carboxylase, which was increased 1.8-fold in MAK.

One note of interest is the change in opposite direction for the transcripts of phosphoglycerate mutase isozyme B (Pgam1) and M (Pgam2). In mammalian tissues, phosphoglycerate mutase exists as a dimer of two distinct 30 kDa subunits, that is, the B form which is expressed ubiquitously and the M form which is expressed abundantly in muscle tissue. In mammalian tissue, the phosphoglycerate mutase MM form, has a higher enzyme activity than the heterodimer BM (expressed in heart) or homodimer BB (Bartrons and Carreras, 1982). In MAK, both phosphoglycerate mutase isoforms are expressed at an average intensity level of ~8000 as detected on the MOE430A array, however upon butyrate exposure the M isoform increased 2.9-fold while B isoform decreased 2.5-fold. The intensity reflects the abundance level of transcripts in reference to other genes probed by the array. The intensity of these two enzymes are in the same range as highly expressed ribosomal genes (ribosomal protein 63, L15, L52) and oxidative phosphor-

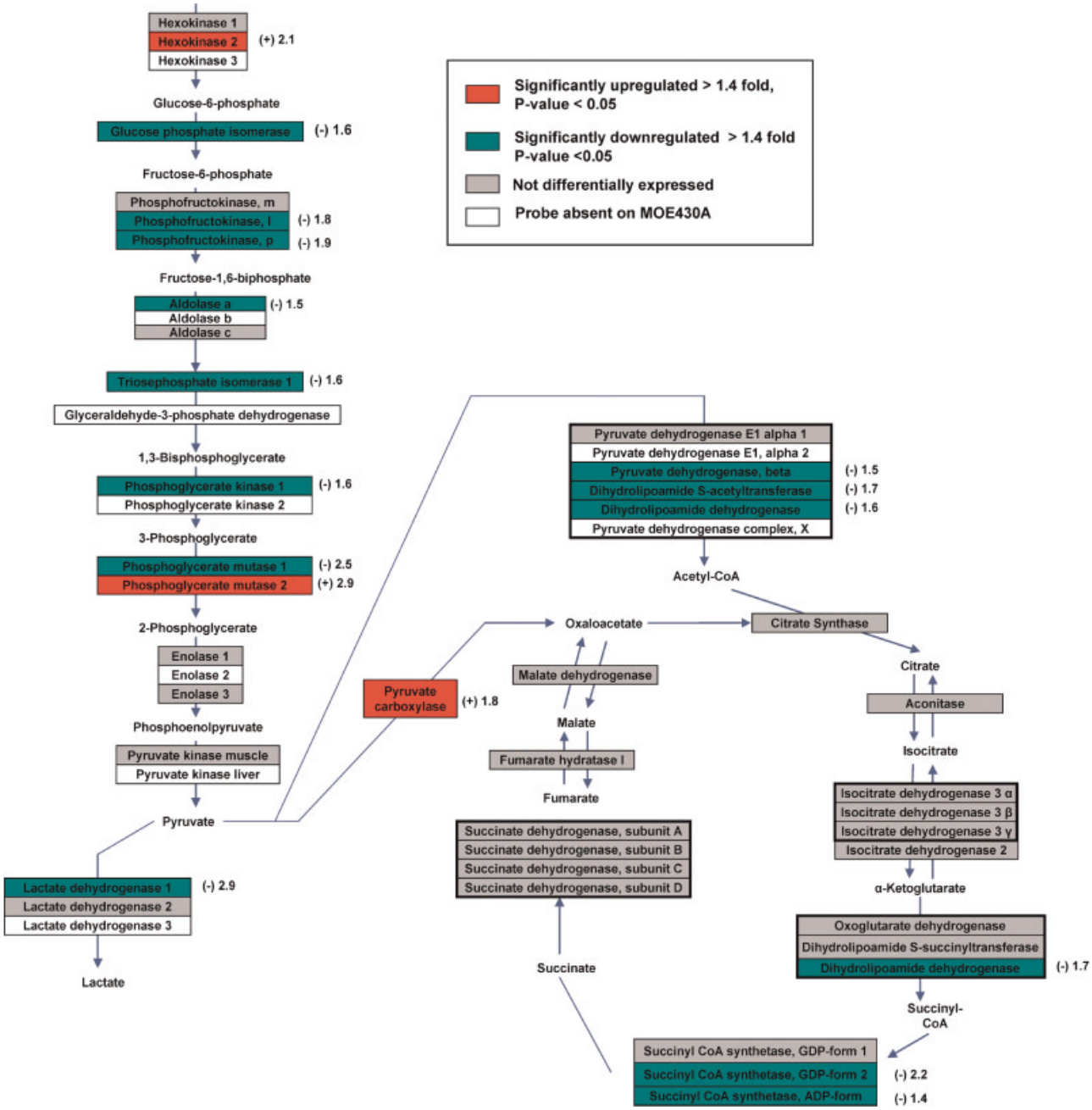

Figure 3. Glycolysis pathway and TCA cycle in MAK colored according to differential expression and statistical criterion. Fold change values for genes that are differentially expressed are listed. [Color figure can be seen in the online version of this article, available at www.interscience.wiley.com.]

ylation genes (cytochrome *c* oxidase VIIa, ubiquinol cytochrome c reductase 1, NADH dehydrogenase Fe-S protein 3).

The probe coverage for glycolysis and TCA cycle genes on the CHO microarray is substantially smaller than that in the mouse array used. Among the gene probes present, triose phosphate isomerase 1, phosphoglycerate kinase 1, malate dehydrogenase, isocitrate dehydrogenase and the subunits of pyruvate dehydrogenase complex were unchanged. Enolase 1 and lactate dehydrogenase 1 were both down-regulated by 1.7-fold. Interestingly, the decrease of lactate dehydrogenase expression was detected in both CHO and MAK, however the glucose consumption and lactate production levels did not change appreciably (data not shown).

Fatty Acid Biosynthesis and Metabolism

Butyrate treatment caused changes in the expression of fatty-acid oxidation genes in both MAK and CHO. The fatty-acid β-oxidation enzymes in MAK with their corresponding fold changes are shown in Figure 4. Fatty acid β-oxidation takes place inside the mitochondria; as such fatty acids with 14 or more carbons must first undergo esterification to become fatty acyl CoA, before being transported into mitochondria (Fig. 4).

Three isoforms of acyl-CoA synthase, which catalyse the thioesterification reaction, are expressed in MAK. Two of them (acyl-CoA synthase 1 and 4) had low expression intensity (<1,000). One of the isoforms expressed at high level, acyl-CoA sythase 5, was decreased 1.9-fold. Following esterification, acyl-CoA is converted to fatty acyl-carnitine by carnitine palmitoyltransferase 1a in the outer mitochondrial membrane. This enzyme increased 1.5-fold in transcript expression, whereas mitochondrial acyl-carnitine translocase, the transporter of acyl-carnitine into the mitochondria was decreased 2.1-fold upon butyrate treatment.

In mitochondria matrix, fatty acyl-CoA first undergoes dehydrogenation to form a double bond. The reaction is catalyzed by four isozymes of acyl-CoA dehydrogenase, each of which reacts with a fatty-acid substrate of a specific chain length. Acyl-CoA dehydrogenase, very long chain (substrate: C_{12} to C_{18} fatty acids), was increased 2.1-fold while the medium chain isoform (substrate: C_4 to C_{16} fatty

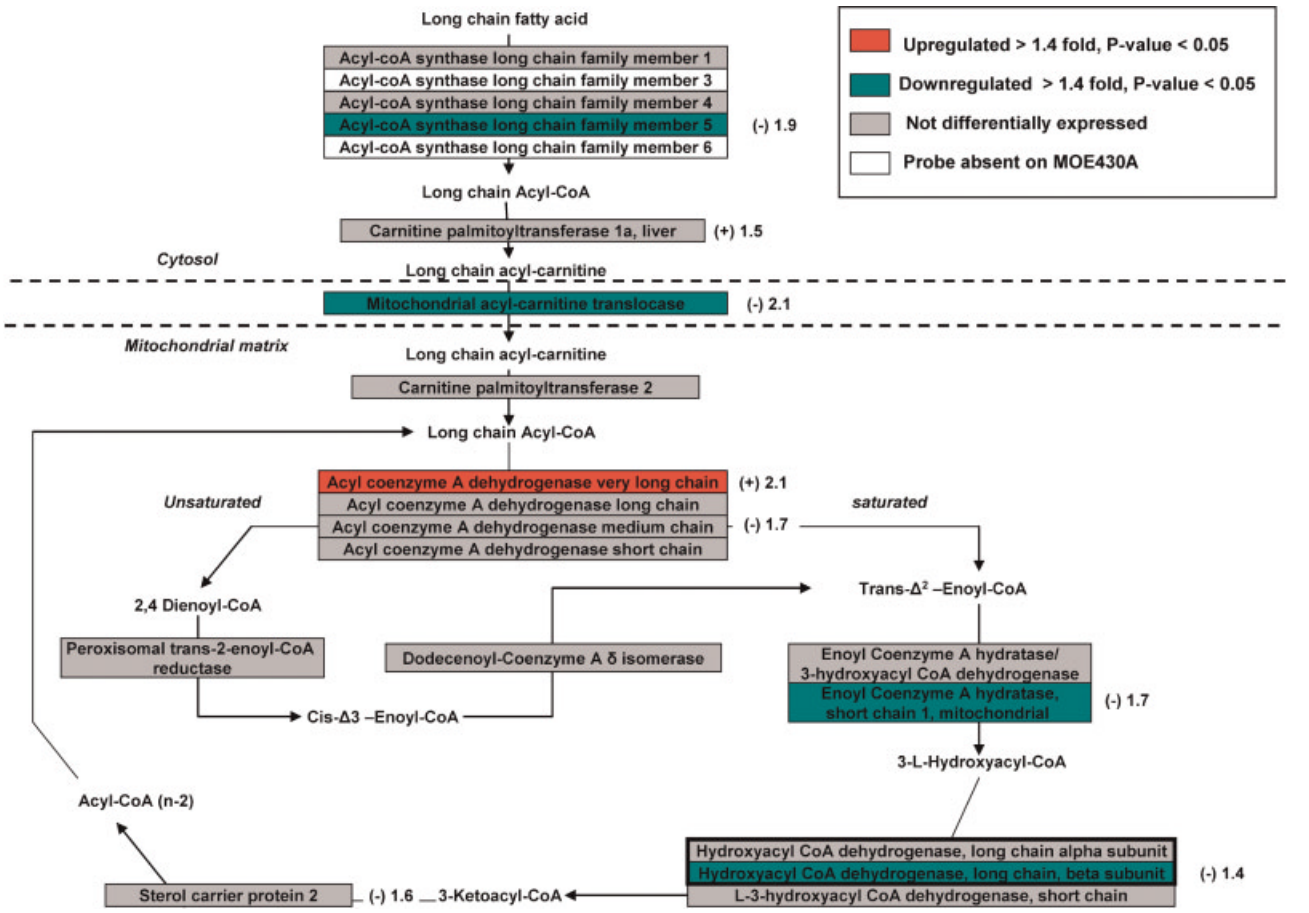

Figure 4. Fatty acid β-oxidation pathway in MAK colored according to differential expression and statistical criterion. Fold change values for genes that met differentially expressed criterion are listed. [Color figure can be seen in the online version of this article, available at www.interscience.wiley.com.]

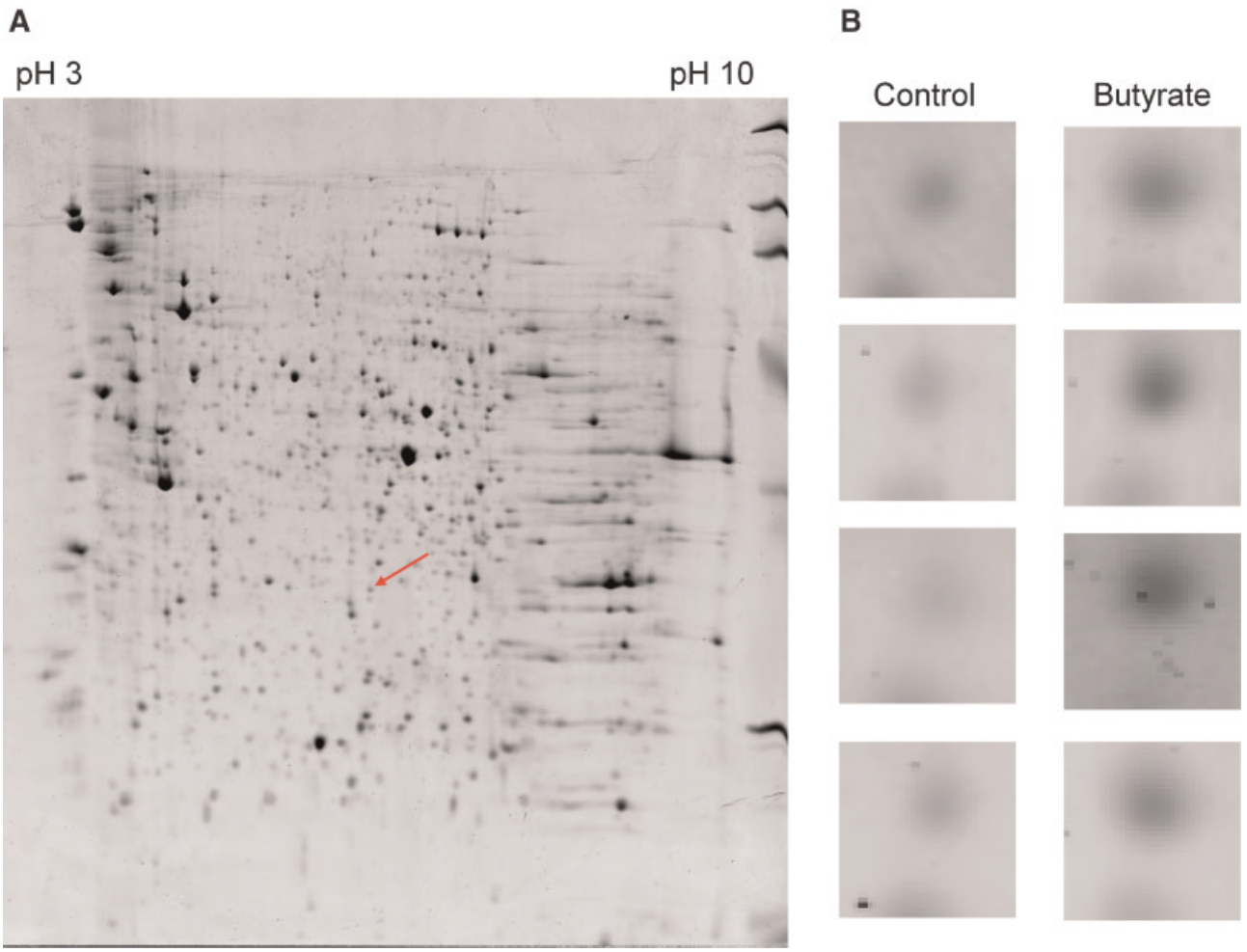

Figure 5. Two-dimensional gel electrophoresis of sodium butyrate treated MAK cells. Protein extracts from MAK cells were separated using 2-DE as described in Materials and Methods. One of four replicate images of sodium butyrate treated MAK cells (**A**). Zoomed region of the image (arrowed) showing four replicate spots from control and sodium butyrate treated MAK cells (**B**). The protein was identified as 60S acidic ribosomal protein P0 (P14869) and having a 3.4-fold higher expression after treatment with sodium butyrate (*P*-value = 4.2E−06). [Color figure can be seen in the online version of this article, available at www.interscience.wiley.com.]

acids) was reduced 1.7-fold (*P*-value of 0.06). The subsequent hydration reaction in the β-oxidation cycle is carried out by enoyl-Coenzyme A hydratase short chain 1. The transcript for this gene was decreased 1.7-fold. The third step of the β-oxidation cycle is catalyzed by L-3 hydroxyacyl coA dehydrogenase. The beta-subunit of the long-chain 3-hydroxyacyl-CoA dehydrogenase decreased by 1.4-fold.

For CHO cells, the β-oxidation gene acetyl-CoA acyltransferase 2 (not shown in Fig. 4) was increased 1.6-fold at the transcript level. Three other fatty acid metabolism genes had their corresponding probes present in the CHO array (carnitine palmitoyltransferase 2, acyl coA dehydrogenase very long chain and dodecenoyl-coA delta isomerase). None was shown to be differentially expressed.

As a 4-carbon short chain fatty acid, butyrate can enter the β-oxidation pathway to form the precursor acetyl-CoA. Butyrate is first converted to butyryl-CoA, and subsequently to enoyl-CoA, L-hydroxyacyl-CoA, and finally acetyl-CoA. Acetyl-coA is one of the important precursor for the TCA cycle and lipid metabolism. A previous study has reported butyrate to be oxidized and incorporated into cellular lipids in human cell lines (Leschelle et al., 2000). In MAK, the decreased transcript expression of β-oxidation genes suggests that butyrate could have a profound effect on slowing down the synthesis of acetyl-CoA from long-chain fatty acid oxidation.

Cholesterol Biosynthesis and Metabolism

Our microarray analysis revealed many genes involved in cholesterol biosynthesis to be differentially expressed in sodium butyrate treated MAK and CHO cells. Out of the 17 cholesterol biosynthesis pathway genes that were probed, six exhibited a negative fold change while two were increased at

the transcript level in MAK cells. Most of the cholesterol biosynthesis pathway genes are represented on the MOE430A and are listed according to their order in cholesterol biosynthesis in Table I. 3-hydroxy-3-methylglutaryl-coA synthase 1 which is involved in the conversion of acetyl-CoA to HMG-CoA was down-regulated by twofold in the butyrate-treated culture. Five other genes, (mevalonate (diphospho) decarboxylase, lanosterol synthase, lanosterol 14-alpha demethylase, C4-methyl sterol oxidase, sterol-C5 desaturase) which are involved in subsequent steps of converting mevalonate-5-pyrophosphate to 7-dehydro cholesterol were also reduced at the transcript level.

Out of eight cholesterol metabolism genes which are represented on the CHO array, four (sterol-regulatory element binding factor 2, farnesyl diphosphate synthetase, squalene epoxidase and C4-methyl sterol oxidase) were reduced at the transcript level with a P-value <0.05 (Data not shown). In addition, lanosterol 14-alpha demethylase was decreased by 1.8-fold at a P-value of 0.1. In general, a decrease of cholesterol biosynthesis transcripts was observed in both MAK and CHO.

Cell Cycle Control

Seventy seven genes represented on the MOE430A chip are involved in cell cycle regulation as annotated in the KEGG database. Among them, 26 were differentially expressed upon butyrate treatment for MAK. With the exception of two cyclin-dependent kinase inhibitor (Cdkn2a, Cdkn1a), cyclin D2 and mitotic arrest deficient homolog 2, the other 22 transcripts decreased over 1.4-fold (Table II). These genes include two cyclin dependent kinases (Cdk2, Cdk4), three cyclins (Ccna2, Ccnb2, CcnG2) and five cell division cycle genes (Cdc3a, Cdc2a, Cdc20, Cdc45l). All these genes interact with other proteins through binding or post-translational modification to regulate specific stages of cell cycle (for review, see (Ekholm and Reed, 2000; Pines, 1995)).

The G1/S phase transition is controlled by the formation of cyclin A2—Cdk2 complex and Cdk2—Cyclin E complex (Dulic et al., 1992; Hinds et al., 1992; Lees et al., 1992). Cyclin dependent kinase inhibitor Cdkn1a provides negative control of cell cycle by inactivating these cyclin-cdk complexes (Harper et al., 1993). In MAK cells, the decrease of Cyclin A2, Cdk2 and Cdk4 transcript in concurrence with the increase of cyclin dependent kinase inhibitor could deter cellular progression through S phase.

From the 15 cell cycle gene orthologs that were present on the CHO array, cyclin D2 and chromosome segregation 1-like shows a similar transcript response to MAK. In contrast, the transcript level of two cell cycle control related genes, telomeric repeat binding factor 1 (Terf1) and chromosome-condensation related SMC associated protein 1 (Ncapd2) changed in opposite direction between CHO and MAK. Both genes exhibited increased transcript levels in CHO but were decreased in MAK. Notably, Terf1 encodes a protein belonging to a component of the telomere nucleoprotein complex. This protein is present at telomeres throughout the cell cycle and functions as an inhibitor of telomerase, to limit the elongation of individual chromosome ends (Chong et al., 1995).

Apoptosis

Sixteen genes involved in apoptosis were differentially expressed in MAK (Table III). Butyrate is known to cause apoptosis, it is thus not surprising to find the increase of five pro-apoptotic transcripts (bcl-2 like 11, caspase 8, tumor necrosis factor superfamily member 10, growth arrest and DNA damage-inducible 45β, apoptosis-associated speck-like protein containing a CARD) and the decrease of four anti-apoptotic genes (baculoviral IAP repeat-containing 3, 5, nuclear factor of kappa light chain gene enhancer in B-cells 1, bcl-2/adenovirus E1B 19 kDa-interacting protein 1, NIP3). Not all pro-apoptotic members displayed positive fold change. Two pro-apoptotic genes belonging to the Bcl2 family—Bcl-2 associated X protein (Bax) and BH3-interacting domain agonist (Bid) were decreased, and so were five apoptotic inducing factors (caspase 3, death associated protein 3, programmed cell death 4, 6, and 8).

Table I. Expression fold changes in cholesterol biosynthesis pathway in MAK and CHO.

		MAK		CHO	
Gene symbol	Gene name	Fold change	P-value	Fold change	P-value
Cholesterol biosynthesis					
Hmgcs1[a]	*3-hydroxy-3-methylglutaryl-CoA synthase 1*	(−) **2.0**	**1.2E−4**	(+) 1.2	4.2E−1
Mvd	*Mevalonate (diphospho) decarboxylase*	(−) **1.6**	**1.0E−2**	NA	
Idi1	*Isopentenyl-diphosphate delta isomerase*	(−) **1.4**	**1.0E−2**	(−) 1.3	1.0E−1
Fdps	*Farnesyl diphosphate synthetase*	(−) 1.1	5.0E−4	(−) **1.7**	**1.0E−2**
Lss	*Lanosterol synthase*	(−) **2.0**	**4.7E−3**	NA	
Cyp51	*Lanosterol 14-alpha demethylase*	(−) **1.4**	**3.3E−2**	(−) 1.8	1.0E−1
Sc4mol	*C4 methyl sterol oxidase*	(−) **2.8**	**3.8E−3**	(−) 1.3	5.0E−2
Sc5d	*Sterol-C5-desaturase (fungal ERG3, delta-5-desaturase) homolog*	(−) **1.6**	**1.8E−2**	(−) 1.1	3.5E−1
Soat1[a]	*Sterol O-acyl transferase 1*	(+) **2.8**	**4.0E−2**	NA	
Srebp1[a]	*Sterol-regulatory element binding protein 1*	(+) **1.5**	**2.0E−2**	NA	

+, positive fold change; −, negative fold change after butyrate treatment; NA, gene probe is not available on the array.
[a]Genes which were similarly upregulated in time course study (de Leon Gatti et al., 2007).

Table II. Expression fold changes in the cell cycle regulation in MAK and CHO.

Gene symbol	Gene name	MAK		CHO	
		Fold change	*P*-value	Fold change	*P*-value
Ccnd2	*Cyclin D2*	**(+) 2.1**	**4.8E−3**	**(+) 1.5**	**2.0E−2**
Csel1	*Chromosome segregation 1—like*	**(−) 1.5**	**3.1E−2**	**(−) 1.5**	**4.0E−2**
Terf1	*Telomeric repeat binding protein*	**(−) 2.7**	**3.8E−3**	**(+) 1.7**	**3.1E−2**
Ncapd2	*Chromosome condensation-related SMC-associated protein 1*	**(−) 1.4**	**4.1E−2**	**(+) 1.4**	**2.3E−2**
Cdkn1a	*Cyclin dependent kinase inhibitor 1a, p21*	**(+) 2.8**	**2.0E−2**	1.0	2.0E−1
Chek1	*Checkpoint kinase 1 homolog*	**(−) 2.0**	**3.2E−2**	(−) 1.1	6.1E−2
Skp2	*S-phase kinase-associated protein 2*	**(−) 2.0**	**1.5E−2**	(+) 1.2	1.1E−2
Ccng2	*Cyclin G2*	**(−) 1.5**	**5.0E−2**	(+) 1.1	3.2E−1
Mad2l1	*Mitotic arrest deficient, homolog—like 1*	**(−) 2.0**	**3.1E−2**	1.0	9.1E−1
Cdc45l	*Cell division cycle 45—like*	**(−) 1.5**	**5.2E−2**	(+) 1.2	2.2E−2
Btg3	*B cell translocation gene 3*	(−) 1.2	2.0E−1	**(+) 1.5**	**1.2E−3**
Ccni	*Cyclin I*	(−) 1.3	2.3E−1	**(+) 1.6**	**2.7E−2**
Tsg101	*Tumor susceptibility gene 101*	1.0	6.0E−1	**(+) 1.9**	**4.1E−2**
Tada2	*Transcriptional adaptor 2*	(−) 1.2	8.5E−1	**(+) 1.5**	**7.2E−3**
Ptma	*Prothymosin alpha*	1.0	7.6E−1	**(−) 1.5**	**3.8E−2**
Apc	*Anaphase promoting complex subunit 10*	NA		**(−) 1.9**	**2.3E−2**
Cdkn3	*Cyclin dependent kinase 3*	NA		**(+) 1.6**	**5.1E−2**
Cdkn2a	*Cyclin dependent kinase inhibitor 2a*	**(+) 1.5**	**5.0E−2**	NA	
Tfdp1	*Transcription factor Dp1*	**(−) 1.6**	**4.9E−2**	NA	
Cdk2	*Cyclin dependent kinase 2*	**(−) 1.7**	**2.5E−2**	NA	
Cdk4	*Cyclin dependent kinase 4*	**(−) 1.5**	**1.4E−2**	NA	
Ccna2	*Cyclin A2*	**(−) 1.7**	**8.9E−3**	NA	
Ccnb2	*Cyclin B2*	**(−) 1.6**	**2.4E−2**	NA	
Cdca3	*Cell division cycle associated 3*	**(−) 1.7**	**1.8E−3**	NA	
Cdca1	*Cell division cycle associated 1*	**(−) 1.5**	**2.6E−2**	NA	
Cdc2a	*Cell division cycle 2 homolog A*	**(−) 1.5**	**1.2E−2**	NA	
Cdc20	*Cell division cycle 20 homolog*	**(−) 2.0**	**4.6E−3**	NA	
Cdc7	*Cell division cycle 7 (S. Cerevisae)*	**(−) 1.7**	**3.8E−2**	NA	
Cenpf	*Centromere autoantigen H*	**(−) 1.7**	**2.0E−2**	NA	
Cenpa	*Centromere autoantigen A*	**(−) 2.2**	**1.2E−2**	NA	
Chek1	*Checkpoint kinase 1 homolog*	**(−) 1.8**	**5.0E−2**	NA	
Chek2	*Checkpoint kinase 2 homolog*	**(−) 2.4**	**1.0E−2**	NA	
Trp53	*Transformation related protein 53*	**(−) 1.7**	**5.0E−2**	NA	

+, positive fold change; −, negative fold change after butyrate treatment; NA, gene probe is not available on the array.

Aside from its direct role in DNA fragmentation, caspase 3 increases the activity of Bax (Panaretakis et al., 2003) and Bid (Woo et al., 1999). Caspase 3 is required for the translocation of programmed cell death 8 (Pdcd8) from its mitochondria compartment to the nucleus where Pdcd8 affects chromosome condensation (Susin et al., 2000). With its role in activating these other pro-apoptotic members, the decreased levels of caspase 3 may result in a decrease in RNA expression of Bax, Bid, and Pdcd8.

The increase of Gadd45β and Bcl2ll11 transcript level in MAK were not observed for CHO. However proapoptotic factor BCL2/adenovirus E1B-19 kDa-interacting protein 1, NIP2 (Bnip2) and antiapoptotic factors: tumor differentially expressed 1 (Tde1), apoptosis inhibitory protein 5 (Aip5), myeloid cell leukemia sequence 1 (Mcl1), exhibited positive fold changes. Bnip2 which is increased 1.9-fold is known to interact with two anti-apoptotic factors, E1B-19 kDa and Bcll2, and induce apoptosis via mitochondria activated pathways (Zhang et al., 2002). Mcl1 and Tde1 are both antiapoptotic genes that are responsible for stimulating tumorigenesis (Bossolasco et al., 2006; Koshikawa et al., 2006).

Protein Processing and Protein Secretion

Among the ontological classes most affected by sodium butyrate treatment is protein processing. Twenty four orthologous genes involved in protein processing, protein secretion and redox control that were differentially expressed in either CHO or MAK are listed in Table IV. Among the 24 genes, five (microsomal glutathione-S-transferase 3, selenoprotein P plasma 1, glutathione-S-transferase alpha 1, eukaryotic translation initiation factor 2-α kinase and glucose regulated protein 78) changed their expression in the same direction in the two cell lines. In addition, two different subunits of the Sec61 translocon complex, subunit gamma and alpha, were increased in MAK and CHO respectively. Another gene, FK506 binding protein also has different isoforms being differentially expressed in the two cell lines.

Also listed in Table IV are genes involved in protein translocation into ER membrane (Sec61a, Sec61g), in protein folding (FK506 binding protein, calreticulin, cyclophilin D, glucose regulated protein 78, Von-Hippel Lindau binding protein1) and protein trafficking (clathrin,

Table III. Expression fold changes in the apoptosis pathway for MAK and CHO.

		MAK		CHO	
Gene symbol	Gene name	Fold change	*P*-value	Fold change	*P*-value
Pdcd4	*Programmed cell death 4*	(−) **2.1**	**2.7E−3**	(−) **1.4**	**1.0E−2**
Pdcd6	*Programmed cell death 6*	(−) **1.7**	**2.4E−2**	(+) 1.2	3.9E−2
Pdcd8	*Programmed cell death 8*	(−) **1.5**	**2.0E−2**	1.0	7.2E−1
Nfkb1	*Nuclear factor of kappa light chain gene enhancer in B-cells 1*	(−) **1.5**	**3.3E−2**	1.0	9.4E−1
Dap3	*Death associated protein 3*	(−) **1.4**	**2.0E−2**	(−) 1.1	2.8E−1
Traf3	*Tnf receptor-associated factor 3*	(−) **1.5**	**3.0E−2**	(−) 1.1	4.6E−1
Bid	*BH3-interacting domain agonist*	(−) **2.1**	**2.8E−2**	(−) 1.3	1.2E−3
Gadd45β	*Growth arrest and DNA-damage-inducible 45β*	(+) **2.3**	**3.0E−3**	(−) 1.1	1.5E−1
Bcl2l11	*Bcl-2 like 11*	(+) **3.4**	**1.3E−2**	1.0	8.9E−1
Pycard	*Apoptosis-associated speck-like protein containing a CARD*	(+) **1.5**	**4.1E−2**	1.0	8.5E−1
Prkdc	*Protein kinase, DNA activated, catalytic polypeptide*	(−) 1.3	6.7E−2	(+) **1.4**	**4.5E−2**
Pdcd6ip	*Programmed cell death 6 interacting protein*	1.0	9.5E−1	(+) **1.5**	**4.1E−2**
Cul2	*Cullin2*	(+) 1.1	2.0E−1	(+) **1.4**	**4.2E−2**
Cul3	*Cullin3*	(−) 1.2	1.4E−1	(+) **1.4**	**2.8E−2**
Api5	*Apoptosis inhibitory protein 5*	(−) 1.2	4.2E−1	(+) **1.4**	**5.1E−2**
Tde1	*Tumor differentially expressed 1*	(+) 1.1	2.4E−1	(+) **1.5**	**2.3E−2**
Mcl1	*Myeloid cell leukemia sequence 1*	(+) 1.1	5.8E−1	(+) **1.5**	**1.2E−4**
Bnip2	*BCL2/adenovirus E1B 19 kDa-interacting protein 1, NIP2*	(−) 1.2	2.1E−1	(+) **1.9**	**5.0E−3**
Pasg	*Proliferation associated SNF-2 like protein*	NA		(+) **1.6**	**3.2E−2**
Bnip3	*BCL2/adenovirus E1B 19 kDa-interacting protein 1, NIP3*	(−) **2.2**	**5.2E−3**	NA	
Bax	*Bcl-2 associated X protein*	(−) **1.6**	**5.4E−3**	NA	
Birc3	*Baculoviral IAP repeat-containing 3*	(−) **2.0**	**1.7E−3**	NA	
Birc5	*Baculoviral, IAP repeat-containing 5*	(−) **1.4**	**5.2E−2**	NA	
Casp8	*Caspase 8*	(+) **2.1**	**4.4E−4**	NA	
Tnfsf10	*Tumor necrosis factor (ligand) superfamily, member 10*	(+) **1.4**	**2.5E−2**	NA	
Casp3	*Caspase 3*	(−) **1.7**	**2.1E−2**	NA	

+, positive fold change; −, negative fold change after butyrate treatment; NA, gene probe not available on the array.

N-ethylmaleimide sensitive fusion protein, gamma, vesicle-docking protein, KDELR endoplasmic reticulum protein retention receptor 3). Some are involved in the regulation of redox balance in the cytosol (glutathione S transferase alpha 1, glutathione S transferase mu) and the endoplasmic reticulum (Ero1-like β, protein disulfide isomerase A6).

Interestingly, five genes known to be involved in ER stress response exhibited a positive fold change. One of the ER chaperone, glucose regulated protein 78, also known as heavy chain immunoglobulin binding protein, was increased in both CHO and MAK. It is induced in response to overloading of unfolded proteins in the ER to prevent aggregation of polypeptide folding intermediates (Morris et al., 1997). Another gene implicated in unfolded protein response is Eif2ak3, which was similarly increased at the transcript level in both cell lines. Its gene product phosphorylates Eif2-alpha kinase, thus attenuating protein translation, and decreasing protein load into the ER (Ma et al., 2002).

X-box binding protein 1 (Xbp-1), another gene which is associated with unfolded protein response in the ER, was increased 1.4-fold in MAK. In the differentiation of B cells to plasma cells, Xbp-1 plays a role by inducing a wide spectrum of secretory pathway genes localized in the ER or Golgi compartment (Shaffer et al., 2004). Eight of these genes: Sec61a, Dnajb9, Dnajc3, Igh-1a, H13, Hspa5, Herpud1 were upregulated in MAK cells upon sodium butyrate treatment (Table IV). Under similar conditions, two genes that belong to this class of XBP-1 induced genes were upregulated in CHO.

Importantly, Table IV clearly illustrates that for both MAK and CHO cells, a majority of the genes involved in the protein processing and secretion pathway that are probed have altered transcript level. Although the specific genes differentially expressed were not completely identical between the two cell lines, their general trend of positive fold change is visible.

Quantitative 2D Gel-Analysis

Two-dimensional gel electrophoresis (pH range 3–10, non-linear gradient) was applied to cellular protein samples of MAK cells. Over 600 spots were detected on the gel with PDQuest image analysis software. On the basis of $\geq$1.5-fold change, 43 protein spots were differentially expressed upon butyrate treatment. These protein spots were excised, destained, and subjected to MS/MS analysis after tryptic digestion. From the 43 protein gel spots, 34 yield protein identification, while 9 failed to be identified from their corresponding mass spectra. In total, 52 proteins were identified with at least two confident peptide matches from the 34 gel spots. Due to co-migration of proteins in the 2D

Table IV. Expression fold changes in protein folding, transport and ER stress response in MAK and CHO.

Gene symbol	Gene name	MAK		CHO	
		Fold change	*P*-value	Fold change	*P*-value
Protein folding					
Hspa5[a,b]	*Glucose regulated protein 78*	**(+) 1.5**	**3.2E−2**	**(+) 1.6**	**5.0E−2**
Ppid	*Cyclophiilin D*	**(−) 1.7**	**1.0E−2**	(−) 1.4	1.2E−1
Fkbp2	*FK506 binding protein 2*	**(+) 1.7**	**2.2E−2**	NA	NA
	FK506 binding protein 3	(−) 1.3	8.0E−2	**(+) 1.4**	**3.8E−2**
Vbp1	*Von-Hippel Lindau binding protein 1*	**(−) 1.8**	**2.1E−2**	**(+) 1.4**	**4.0E−2**
Tcp1b	*T-complex protein 1, Beta*	(−) 1.0	9.0E−1	**(+) 1.6**	**1.5E−2**
Trap1	*Traf and TNF receptor associated protein 1*	**(−) 1.5**	**4.8E−2**	(−) 1.2	1.1E−1
Grpel1	*GrpE-like 1, mitochondrial*	1.0	1.6E−1	**(+) 1.4**	**9.5E−3**
Calr	*Calreticulin*	**(+) 1.5**	**3.4E−2**	NA	
Dnajc3[a]	*Dna J (HSP40) homolog subfamily C, 3*	**(+) 1.7**	**1.0E−2**	NA	
Dnajb9[a]	*Dna J (HSP 40) homolog subfamily B, 9*	**(+) 2.2**	**9.1E−3**	NA	
Protein trafficking					
Sec61[a]	*Sec61a1*	**(+) 1.5**	**1.0E−2**	NA	NA
	Sec61g1	(+) 1.2	3.4E−1	**(+) 1.8**	**2.0E−2**
Gsn	*Gelsolin*	**(+) 2.4**	**8.2E−3**	(+) 1.1	9.0E−2
Vdp[a]	*Vesicle docking protein, p115*	(+) 1.3	1.0E−2	**(+) 1.5**	**4.8E−2**
Napg	*N-ethylmaleimide sensitive fusion protein γ*	(−) 1.2	3.2E−1	**(+) 1.6**	**1.0E−2**
Clta	*Clathrin polypeptide light chain*	(−) 1.1	4.1E−1	**(+) 1.5**	**6.1E−2**
Arf1	*ADP-ribosylation factor like 1*	1.0	5.6E−1	**(+) 1.6**	**3.8E−2**
Timm8b	*Translocase of inner mitochondrial membrane 8*	**(−) 1.4**	**3.0E−2**	**(+) 1.4**	**1.3E−2**
Tim10b	*Translocase of inner mitochondrial membrane 10b*	NA		**(+) 1.7**	**1.8E−3**
Ap1g1	*Adaptor protein complex AP-1, γ subunit*	NA		**(+) 1.7**	**1.7E−2**
Gga3	*Golgi associated, gamma adaptin ear containing 3*	NA		**(+) 1.6**	**1.0E−2**
Kdelr3	*KDEL endoplasmic reticulum protein retention receptor 3*	**(+) 1.7**	**2.5E−2**	NA	
H13[a]	*Histocompatibility 13*	**(+) 1.6**	**1.1E−2**	NA	
Redox control					
Ero1lb	*Ero1-like Beta (S. Cerivisea)*	**(+) 1.6**	**2.0E−4**	NA	
Prdx5	*Peroxiredoxin 5*	**(+) 1.6**	**2.0E−2**	(+) 1.4	1.0E−1
Pdia6	*Protein disulfide isomerase associated 6*	**(+) 1.4**	**2.0E−2**	(+) 1.1	2.2E−1
Mgst3	*Microsomal glutathione-S-transferase 3*	**(+) 1.6**	**4.0E−2**	**(+) 1.5**	**1.5E−2**
Sepp1	*Selenoprotein P, plasma 1*	**(+) 2.7**	**1.4E−2**	**(+) 1.5**	**8.0E−2**
Gsta1	*Glutahione S transferase α 1*	**(+) 1.4**	**1.0E−2**	**(+) 1.5**	**1.0E−2**
Gstm	*Glutathione S transferase υ 5*	(+) 1.2	3.4E−1	**(+) 1.6**	**1.4E−02**
	Glutathione S transferase υ 1	**(+) 2.2**	**1.5E−3**	NA	NA
ER Stress response					
Eif2ak3	*Eukaryotic initiation factor 2 alpha kinase 3*	**(+) 1.8**	**2.0E−2**	**(+) 1.5**	**2.0E−2**
Ddit3	*DNA damage inducible transcript 3*	**(+) 1.6**	**1.0E−2**	NA	
Herpud1[a]	*Homocysteine inducible, ER stress inducible, ubiquitin like domain 1*	**(+) 1.9**	**1.1E−2**	NA	
Sdf2l1	*Stromal cell derived factor 2 like 1*	(+) 1.1	1.6E−1	**(+) 1.6**	**3.1E−2**
Xbp1	*X-box binding protein 1*	**(+) 1.4**	**4.0E−2**	(−) 1.1	3.3E−1
IgG					
Igh-1a[a]	*Iimmunoglobulin kappa chain variable 8 (V8)*	**(+) 3.8**	**1.0E−2**	NA	
Igk-V21	*Immunoglobulin kappa chain variable 21*	**(+) 1.7**	**1.3E−2**	NA	
Vesicle formation					
Pitpn	*Phosphatidylinositol transfer protein*	(+) 1.2	4.0E−2	**(+) 1.7**	**4.0E−2**
Pld3	*Phospholipase D3*	**(+) 2.3**	**3.8E−3**	NA	

+, positive fold change; −, negative fold change after butyrate treatment.
[a]Genes which are regulated by X-box binding protein 1 (Shaffer et al., 2004).
[b]Genes upregulated in time course study (de Leon Gatti et al., 2007).

gel electrophoresis, more than one protein was identified in 11 protein gel coordinates. These proteins are listed with a co-migration protein ID in Table V.

Out of the 52 unique proteins identified, 22 were increased and 30 had reduced levels upon butyrate treatment. Except for one protein (ZW10, centromere/kinetochore protein) which had a >10-fold increase, all of the other proteins were differentially expressed in the range of 1.6- to 4.4-fold. ZW10 is a protein responsible for proper chromosome segregation during cell division (Starr et al., 1997). The protein is also associated with microtubule dynein, assisting in cargo transport in the Golgi, endosome, and lysosome compartments (Varma et al., 2006).

The biological function for each of the other proteins was assigned in Table V. Overall, proteins that were highly affected by sodium butyrate belong to a class of cytoskeleton

Table V. Differentially expressed proteins identified from MAK cells and separated by 2-DE.

Co-migrating protein IDs	Biological function	Accession	Description	Proteomic results		Microarray results	
				Fold change	*P*-value	Fold change	*P*-value
	Nucleotide biosynthesis	P24547	Inosine-5'-monophosphate dehydrogenase 2	(−) 3.6	1.3E−4	(−) 1.4	6.0E−3
1		Q9DCL9	Phosphoribosylaminoimidazole carboxylase	(+) 2.7	4.0E−3	(−) 1.5	6.0E−3
2		P46664	Adenylosuccinate synthetase, non-muscle isozyme	(−) 3.0	3.0E−2	(−) 1.2	2.4E−1
3		Q9JKX6	ADP-sugar pyrophosphatase	(−) 1.7	2.2E−4	(−) 1.5	2.4E−2
4		Q9D7Y0	Bisphosphate 3'-nucleotidase 1	(+) 1.9	7.6E−5	(−) 1.6	3.4E−2
	Cytoskeleton	Q920C7	Carnitine deficiency-associated protein (CDV3B)	(−) 2.3	4.0E−4	(−) 1.5	7.1E−3
4		P60710	Actin, cytoplasmic	(+) 1.9	7.6E−5	(+) 1.1	2.2E−1
1		P26041	Membrane-organizing extension spike protein	(+) 2.7	4.0E−3	(−) 1.1	3.9E−1
		P68369	Tubulin alpha-1 chain	(+) 3.2	2.8E−2	(+) 1.3	7.9E−2
5		P70441	Ezrin-radixin-moesin binding phosphoprotein 50*	(+) 3.5	7.2E−2	NA	
		P26040	Ezrin, p81 (cytovillin)	(+) 3.0	1.2E−5	(+) 1.1	7.6E−1
6	Signal transduction	Q9JIF0	Protein arginine N-methyltransferase 1	(−) 2.0	2.1E−2	(−) 1.4	2.5E−2
		P13353	Serine/threonine protein phosphatase 2A*	(−) 2.2	2.1E−1	(−) 1.3	1.8E−1
7		Q9EQH2	Adipocyte-derived leucine aminopeptidase precursor	(+) 3.1	1.6E−2	(−) 1.4	1.0E−1
	Cholesterol metabolism	Q8JZK9	3-hydroxy-3-methylglutaryl-coenzyme A synthase 1	(−) 2.4	9.8E−6	(−) 2.1	1.0E−3
1		Q99J08	SEC14-like protein 2	(+) 2.7	4.0E−3	(+) 1.7	6.0E−3
		Q920E5	Farnesyl diphosphate synthetase	(−) 2.4	2.2E−2	(−) 1.2	1.2E−2
8	Glycolysis	P17751	Triosephosphate isomerase	(−) 2.4	6.8E−3	(−) 2.5	2.0E−3
9		O70250	Phosphoglycerate mutase 2	(+) 3.1	2.8E−3	(+) 2.4	2.0E−3
2		P17182	Alpha enolase	(−) 3.0	3.0E−2	(−) 1.2	5.3E−2
	Protein folding	Q91YN9	BCL2-associated athanogene 2	(−) 4.4	4.5E−3	(−) 2.3	4.0E−3
		Q9QZH3	Peptidyl-prolyl cis-trans isomerase E	(−) 1.6	2.0E−3	(−) 1.3	1.0E−2
10		Q8CAY6	T-complex protein 1	(−) 2.2	1.0E−2	(−) 1.0	8.2E−1
2	Protein translation	Q9D8N0	Elongation factor 1-gamma	(−) 3.0	3.0E−2	(−) 1.1	1.5E−1
		P20415	Eukaryotic translation initiation factor 4E	(−) 2.3	3.9E−5	(−) 1.5	8.0E−2
		P14869	60S acidic ribosomal protein P0 (L10E)	(+) 3.4	4.2E−6	NA	
	Chromosome organization	Q921H3	ZW 10, centromere kinetochore protein	> (+) 10	2.7E−7	(−) 1.0	3.3E−1
		Q8R2U5	Ard1 protein	(−) 2.1	1.1E−2	(−) 1.5	5.1E−2
10	Fatty acid metabolism	Q91V12	Cytosolic acyl coenzyme A thioester hydrolase	(−) 2.2	1.0E−2	(−) 1.1	2.9E−1
11		P97823	Acyl-protein thioesterase 1	(+) 2.8	6.1E−4	(−) 1.2	3.9E−1
5	Oxidative stress response	P51855	Glutathione synthetase*	(+) 3.5	7.2E−2	(+) 1.1	2.4E−2
6		Q9CQM9	Thioredoxin-like protein 2	(−) 2.0	2.1E−2	(−) 1.3	1.1E−1
	Protein degradation	Q9R1P0	Proteasome subunit alpha type 4	(−) 2.2	1.5E−2	(−) 1.3	6.0E−2
		Q9JMA1	Ubiquitin carboxyl-terminal hydrolase 14*	(−) 2.1	1.7E−1	(−) 1.1	1.6E−1
	Phosphosulfate biosynthesis	Q60967	Bifunctional 3'-phosphoadenosine 5'-phosphosulfate synthethase 1	(+) 3.2	2.7E−3	NA	
3	Spermidine synthesis	Q64674	Spermidine synthase	(−) 1.7	2.2E−4	(−) 1.1	3.8E−1
	Apoptosis	Q8BU13	Proapoptotic caspase adaptor protein	(−) 2.3	2.6E−2	NA	
	Cell cycle	P14701	Translationally controlled tumor protein	(−) 4.0	2.6E−2	(+) 1.0	1.2E−1
	Development	Q9ERE7	Mesoderm development candidate 2	(−) 2.3	1.2E−2	(−) 1.3	8.1E−2
5	DNA repair	Q9WTM5	RuvB-like 2*	(+) 3.5	7.2E−2	(−) 1.4	1.0E−2
9	Electron transfer	Q9DCW4	Electron transfer flavoprotein beta-subunit	(+) 3.1	2.8E−3	(+) 1.1	5.0E−2
	Lipid biosynthesis	Q922E4	Ethanolamine-phosphate cytidylyltransferase	(−) 2.0	9.9E−4	(−) 1.1	8.1E−2
3	Phosphate metabolism	Q8BTY3	Inorganic pyrophosphatase	(−) 1.7	2.2E−4	NA	

Table V. (*Continued*)

Co-migrating protein IDs	Biological function	Accession	Description	Proteomic results		Microarray results	
				Fold change	*P*-value	Fold change	*P*-value
3	mRNA processing	Q62093	Splicing factor, arginine/serine-rich 2	(−) 1.7	2.2E−4	(−) 1.4	7.0E−2
7	Protein processing	Q9DBP9	Mitochondrial Lon protease homolog	(+) 3.1	1.6E−2	(−) 1.2	1.0E−1
	Protein transport	Q9DBG5	Mannose-6-phosphate receptor-binding protein 1	(+) 2.1	5.9E−3	(+) 1.6	1.1E−2
1	TCA cycle	O88844	Isocitrate dehydrogenase	(+) 2.7	4.0E−3	(+) 1.1	5.1E−1
11	Viral life cycle	Q64033	Antigen LEC-A	(+) 2.8	6.1E−4	(+) 1.0	6.6E−1
	Other proteins	Q9CYW4	Haloacid dehalogenase-like hydrolase domain containing 3	(+) 2.0	4.4E−3	(+) 1.0	5.3E−1
2		O88712	C-terminal binding protein 1	(−) 3.0	3.0E−2	(−) 1.3	9.0E−2
		Q8BK16	Sperm-associated antigen 7	(−) 2.3	2.8E−4	(−) 1.5	2.6E−2
8		Q8R2U4	UPF0351 protein C9orf32	(−) 2.4	6.8E−3	NA	

In a number of cases (shown with a co-migrated protein ID) multiple proteins were found to co-migrate in a single spot. Results from protein analysis are compared with parallel studies conducted with microarray analysis.

NA, gene probe not present on Affymetrix MOE430A array.

*P-value >0.05, analyzed by student's t-test on four gel replicates.

elements (with six proteins) and nucleotide biosynthetic enzymes (with five proteins). This is followed by proteins involved in signal transduction, cholesterol metabolism, glycolysis, protein folding and protein translation with three proteins differentially expressed in each class.

Among the identified cytoskeleton re-organization proteins, ezrin (p81) and ezrin-radixin-moesin (ERM) binding phosphoprotein 50 (Slc9A3R1) were increase by more than threefold. Ezrin, belonging to the family of ezrin-radixin-moesin (ERM) complex, is one of the important linkers between integral membrane and cytoskeletal proteins. ERM binds to actin in specialized plasma membrane structures, and is involved in cell morphogenesis and adhesion (Mangeat et al., 1999). Of interest the conformation of ERM is found to be stabilized through binding to Slc9A3R1. Additionally, cytoplasmic actin, which increased 1.9-fold at the protein level, has also been implicated to bind to the ERM complex (Lozupone et al., 2004).

Three purine biosynthetic proteins (Impdh2, Paics, and Adss2) were also identified in the quantitative 2D gel. One of the purine metabolism proteins, Impdh 2, decreased by 3.6-fold and encodes the rate limiting enzyme in the de novo guanine nucleotide biosynthesis. The protein is involved in maintaining guanine deoxy- and ribonucleotide pools required for DNA and RNA synthesis. Two other purine metabolism proteins, Adss2 and Paics, are differentially expressed in opposite trends. Both proteins are involved in converting L-aspartate to different purine nucleotide precursors. The increase of one enzyme level versus the decrease in the other could indicate L-aspartate is preferentially directed towards the synthesis of one particular purine intermediate.

Compared to that of MAK cell samples, the proteomic analysis of CHO cells did not yield as many differentially expressed proteins. Over 400 protein spots were resolved on the gel, and amongst these spots, 34 were identified to be differentially expressed. In total, 21 out of the 34 protein spots yield confident protein identifications (Table VI). Except for three proteins identified based on hamster sequences, the others were all identified based on cross-species identification to other mammalian orthologs.

Similar to MAK, one of the most abundant gene classes affected by butyrate in CHO at the protein level belong to a class of cytoskeleton elements. Gelsolin which was increased 2.4-fold in MAK transcript level was upregulated 2.3-fold at the protein level in CHO. This gene is recognized as an actin severing element that restructures actin cytoskeletons. Modulation of the actin complex by the severing and capping action of gelsolin, represent a mechanism for some cell lines in regulating secretion (Beaulieu et al., 2005). On a similar note, another proteomic study on gene-amplified CHO clones expressing secreted alkaline phosphatase (SEAP) had identified four cytoskeletal proteins to be increased along with SEAP productivity levels (Hayduk and Lee, 2005). One of the proteins identified, actin capping protein α1 (CAPZ) plays a similar role to gelsolin, which alters the dynamics of actin polymerization. Another protein identified by Hayduk and Lee is ezrin (cytovillin 2) which has been shown in CHO to have a twofold decrease in protein level upon butyrate treatment (Table VI). Taken together, these proteomic studies suggested that a family of actin reorganizing proteins could play an important role in protein secretion.

Comparison of Proteomic and Transcriptome Results of MAK and CHO

As seen in Table V, 46 of the MAK proteins identified have a corresponding gene sequence on the MOE430A array (Table V). Eleven of these proteins which changed in the same direction as their corresponding transcript were also called differentially expressed with >1.4-fold and P-value <0.05. An additional six proteins agree with the direction of

Table VI. Differentially expressed proteins identified from CHO cells and separated by 2-DE.

Comigrating protein IDs	Biological function	Accession	Description	Proteomic results		Microarray results	
				Fold change	*P*-value	Fold change	*P*-value
	Cytoskeleton	P06396	Gelsolin precursor, plasma	(+) 2.3	1.6E−02	(−) 1.1	3.4E−1
		Q7TQ35	CAP1 protein	(+) 2.4	2.3E−03	(+) 1.0	6.0E−1
		P26040	Ezrin (p81) (cytovillin) (Villin 2)	(−) 2.0	4.0E−05	NA	
	Fatty acid beta-oxidation	Q61425	Short chain 3-hydroxyacyl-CoA dehydrogenase, mitochondrial precursor	(+) 2.6	2.6E−02	(+) 1.2	7.0E−1
		P14604	Enoyl-CoA hydratase, mitochondrial precursor	(+) 2.7	4.5E−02	NA	
		Q9WTL7	Acyl-protein thioesterase 2	(+) 1.9	2.0E−02	NA	
	Nucleotide metabolism	P00375	Dihydrofolate reductase	(+) 3.7	1.3E−03	(+) 1.7	0.01
		Q922W5	Pyrroline-5-carboxylate reductase 1	(+) 2.7	8.2E−03	NA	
	Sterol carrier	P22307	Nonspecific lipid-transfer protein, mitochondrial precursor	(+) 2.0	1.4E−03	NA	
	Apoptosis	P20333	Tumor necrosis factor receptor superfamily member 1B precursor	(+) 4.4	2.4E−02	NA	
	Calcium ion binding protein	Q96PQ8	Factor VII active site mutant immunoconjugate	(+) 3.0	3.4E−03	NA	
	Cell cycle	P11440	Cell division control protein 2 homolog	(+) 1.8	5.9E−04	NA	
	Cholesterol metabolism	P13704	Hydroxymethylglutaryl-CoA synthase, cytoplasmic	(−) 2.2	1.2E−03	(+) 1.2	4.4E−1
	ER stress response	Q9ESP1	Stromal cell-derived factor 2-like protein 1 precursor	(+) 1.9	2.0E−04	(+) 1.6	3.0E−2
	Protein degradation	Q9Z2U0	Proteasome subunit alpha type 7	(+) 2.0	1.8E−02	(+) 1.5	4.1E−2
	Protein metabolism	Q8BPW9	Aspartyl aminopeptidase	(+) 2.5	7.2E−03	NA	
	Modification of sulfur-containing enzymes	P46635	Thiosulfate sulfurtransferase	(+) 2.1	1.2E−03	NA	
1	Nucleocytoplasmic transport/ cell cycle	P17080	GTP-binding nuclear protein RAN (TC4)	(+) 2.1	1.2E−03	NA	
1	Zinc ion binding protein	Q60866	Phosphotriesterase related protein	(+) 2.2	6.4E−03	NA	
	Translation	Q8BFR5	Elongation factor TU	(+) 2.3	4.7E−02	NA	
	Unknown	Q922L5	Staphylococcal nuclease domain containing 1	(+) 1.6	2.3E−02	NA	

In one case two proteins were found to co-migrate in a single gel spot (shown with identical co-migrated protein ID). Results from protein analysis are compared with parallel studies conducted with microarray analysis.

NA, gene probe not present on CHO cDNA array.

RNA expression change; however the transcript although had high statistical confidence (P-value <0.05), did not meet the >1.4-fold criterion to be called differentially expressed. In contrast to these 17 genes, only three showed an opposite change in differential expression between transcript and protein. Although the number of proteins identified were too few to reach a definite conclusion, overall we find there is a good agreement between the transcript and protein fold changes in MAK.

The ER chaperones increased at the transcriptome level (Grp78, FK506bp2, Calr, and Dnajb9) were not amongst the differentially expressed proteins identified in the 2D gel. The inherent limitations in membrane protein detection by two-dimensional gel electrophoresis may have contributed to the descrepancy (Santoni et al., 2000). However three protein chaperones were decreased at the protein level, all of them localized in the cytosol (T-complex protein 1, Bcl-2 athanogene2) or the nucleus (Peptdiyl-prolyl-cis-trans isomerase E). Decrease of Bcl-2 athanogene 2 at the mRNA and protein level were detected. This protein is a chaperone regulator that binds to the ATPase domain of cytosolic heat shock protein 70 to inhibit its chaperone activity. Decrease of this protein by fourfold may imply the release of inhibition on heat shock protein 70. Hence, this agrees with the observed trend that protein processing activity were increased in MAK by butyrate.

Comparing the response of CHO cells at transcriptome and proteome levels is a more difficult task as many of the proteins identified do not have a corresponding probe on the microarray. The majority of the differentially expressed proteins (19 out of 21) were upregulated. Among the seven genes which have a corresponding probe represented on the CHO microarray four did not show evidence of differential expression at the transcript level, while three showed a similar upregulation in both transcript and protein levels.

Discussion

In this study we employed species-specific DNA microarrays to probe for gene expression changes in CHO and MAK under sodium butyrate treatment. Since transcriptional changes do not necessary reflect the response at the protein level, we also investigated proteomic changes by quantitative 2-dimensional gel electrophoresis. The absence of a large protein dataset for the hamster species did not hinder the identification of differentially expressed proteins (21 out of the 34 protein spots were identified). Other groups have also reported successful cross-species identification on CHO proteins (Baik et al., 2006; Van Dyk et al., 2003). This is likely made possible by the high degree of conservation in protein sequences between Chinese hamster, mouse, rat, and human.

The number of proteins found to be differentially expressed was relatively small for both CHO and MAK. The protein detection sensitivity, the pH range probed, and the intrinsic limitation of the method used in isolating membrane associated proteins, may have all contributed to this small number of differentially expressed proteins. The limitations in protein detection on 2D-gel electrophoresis when compared to microarray results have been similarly reported in the studies of cholesterol dependence in myeloma cells (Seth et al., 2005) and of metabolic shift in MAK cells (Korke et al., 2004). Improvement in the number of differentially expressed proteins identified can be made by employing non 2D gel techniques, specifically stable isotope peptide labeling for different protein samples followed by LC/MS-MS identification.

In a previous study utilizing a prototype cDNA array with smaller gene coverage, the time course effect of butyrate on the transcriptome of MAK and CHO were examined (de Leon Gatti et al., 2007). It was observed that the transcriptome changes were affected most profoundly 27 h after the initiation of butyrate treatment. Hence, 27 h was chosen for transcriptome profiling in this study. In addition to using microarrays with expanded gene coverage, this study compared transcriptome of 1 mM butyrate treated and non-treated cells at 27 h, rather than between cells treated for 27 h and untreated at 0 h timepoint. In the previous study (de Leon Gatti et al., 2007), differential expression could also be merely due to the effects of time course in culture. Consistency of differential expression between the two studies will give further credence of genuine effects of butyrate. This consistency was observed in MAK for three cholesterol metabolism genes (Soat, Hmgcs1, Srebp1) two glycolysis genes (Ldha, Pgam1), and a protein folding chaperone (Hspa5). Similarly, in CHO the glycolysis gene Ldha, and protein folding chaperone Hspa5 were differentially expressed in a consistent trend in both studies.

Interestingly, in both studies a higher number of genes were called differentially expressed in MAK than in CHO. By comparing the expression of orthologous probes between the CHO and mouse array, a higher magnitude of fold change were detected amongst the differentially expressed genes in MAK compared to CHO. This may reflect the difference in their sensitivity to butyrate. The concentration of butyrate which gave rise to the highest increase of specific antibody productivity was 2 mM in CHO and 1 mM in MAK (de Leon Gatti et al., 2007). However, to avoid the decreased viability interfering with the transcriptome and proteome analysis, both MAK and CHO cells were treated with the lower 1 mM butyrate.

Butyrate Effects on Cell cycle and Apoptosis

Butyrate is well known to interfere with cell cycle regulation and apoptotic pathways in mammalian cells. 26 and 10 cell-cycle related genes met our differential expression criterion in MAK and CHO respectively. A substantial fraction of these genes regulate cell cycle through a variety of mechanisms that leads to the inhibition of RNA translation or DNA replication. In MAK, the negative fold change of cyclin A2, cyclin B2 and two cyclin dependent kinases suggested a downregulation of cell cycle progression by butyrate. Similarly in CHO cells, three anti-proliferative genes, B-cell translocation gene 3, tumor susceptibility gene 101 and cyclin dependent kinase 3 were also upregulated. Of interest, cyclin D2 is upregulated in both MAK and CHO cells. In another investigation, Cyclin D3, a homolog of cyclin D2 has been similarly upregulated in human colon carcinoma cells upon butyrate addition (Leschelle et al., 2000).

Since cell cycle regulation and apoptosis are integrated in the cellular signaling framework, it was not surprising to also find apoptosis-related genes to be differentially expressed in both MAK and CHO in response to butyrate. For MAK cells, 16 apoptotic genes were differentially expressed. These include the increase of five pro-apoptotic genes (Bcl2l11, Casp8, Tnfsf10, Gadd45β, Pycard) and reduced transcript levels of four anti-apoptotic genes (Birc3, Birc5, Nfkb1, Bnip3). Interestingly, not all pro-apoptotic gene members showed positive fold changes, as we also found seven pro-apoptotic genes to have lower expression level. Specifically, two members of Bcl-2 family (Bix, Bad) and one caspase (Casp3) decreased $\geq$1.4-fold (Table III). The negative fold change in these transcripts might suggest a cellular defense response to elevated apoptosis.

Butyrate Effects on Protein Processing and Secretion Genes

From the transcriptome analysis, we found butyrate has a large effect on protein processing genes in both MAK and CHO. Specifically, the upregulation of glucose regulated protein 78 (GRP78), elongation initiation factor 2 alpha kinase and three redox balance genes were detected in both cell lines. Additionally, the light chain component of IgG, was upregulated 3.8-fold in MAK. We postulate this higher level of IgG transcript leads to a higher protein load in the endoplasmic reticulum, triggering the downstream expres-

sion of these genes. Interestingly, a separate study found GRP78 to be upregulated when synthesis of heterologous Factor VIII was increased in CHO cells after sodium butyrate treatment (Dorner et al., 1989).

Apart from protein processing in the endoplasmic recticulum, the functional class of genes involved in vesicle transport was also upregulated in CHO following butyrate treatment. One of these upregulated genes, vesicle docking protein (Vdp) is essential for the biogenesis of the Golgi apparatus (Alvarez et al., 1999). Vdp interacts with Golgi-localized SNARE proteins to enhance vesicle complex formation. The upregulation of phospholipid transfer protein (Pitpn) also suggested increased vesicle transport in CHO. This gene is known to promote the budding of nascent secretory vesicles from the trans-Golgi network by modulating phospholipid metabolism (Ohashi et al., 1995). Additionally, two other genes which were upregulated in CHO: clathrin and N-ethylmaleimide sensitive fusion protein gamma are required for vesicle fusion and vesicle recycling (Blondeau et al., 2004; Larance et al., 2005).

The above mentioned genes were not differentially expressed in MAK, however we identified two protein trafficking genes that were upregulated. One of the gene, KDEL endoplasmic reticulum protein retention receptor 3, is involved in ER to golgi vesicle mediated transport (Yamamoto et al., 2001). The second gene, phospholipase D3, is a phospholipid-modifying enzyme which has been implicated in vesicle trafficking (Exton, 1997). Specifically, phospholipase D can modulate cellular levels of phosphatidylcholine and phosphatidic acid, which enhances the formation and release of secretory vesicles by altering local charge distribution on the Golgi membrane.

In general, transcript changes related to vesicle mediated transport were observed in CHO and MAK upon butyrate treatment. Our microarray findings were in concordance to an electron microscopy study showing that hybridoma clones with high antibody productivity titer have an abundance of vesicular-tubular structures in the endoplasmic reticulum (al-Rubeai et al., 1990). Given that butyrate enhances specific production of IgG in CHO and MAK, our transcriptome analysis suggested that this was not only a result of higher IgG transcript but also due to elevated levels of ER protein processing genes in co-ordination with the upregulation of redox balance and vesicle transport activity.

Concluding Remarks

In the past decade the productivity of mammalian cell based bioprocesses has increased drastically. However, the increasing demand and continued arrival of new products has necessitated the drive to increase the productivity even higher. A better understanding of the gene-trait relationship of hyperproductivity will certainly facilitate the development of designer cell lines. Various approaches have been taken to increase our knowledge of the complex trait of hyperproductivity. Drawing insight from the differentiation of B cells to become secretory plasma cells (Romijn et al., 2005; van Anken et al., 2003) comparing clones of different productivity (Dinnis et al., 2006; Seth et al., 2006) and probing culture conditions that increase the productivity will enhance our understanding. Through this combined profiling of transcriptome and proteome of two cell lines undergoing the same butyrate treatment, we looked for common threads in their response to butyrate. Overall, metabolic genes were affected, especially in MAK, but no consistent trend was apparent in both CHO and MAK. On the other hand, the perturbation seen on genes involved in cell cycle, apoptosis and protein processing show some consistent behavior between the two cell lines. The effect of butyrate on cell cycle and apoptosis has been known and thus is not surprising. What is most interesting is the common up-regulation of genes involved in vesicle trafficking for the protein secretion pathway. The secretion of antibody is mediated through vesicles after completion of glycosylation in Golgi. The vesicle membrane after being incorporated into cytoplasmic membrane needs to be recycled to maintain membrane and organelle homeostasis. A high producer is thus likely to have a higher vesicle traffic and membrane recycling activity. The observed results are consistent with the physiological needs of the cell. In this study, although we also observed consistent expression level changes between the two cell lines, a more prevailing observation is a general change in the same pathway, rather than the same genes. The pathways perturbed, cell cycle, apoptosis and protein secretion are very complex with many components serving overlapping functions. Thus, there might be different combinations of expression profile change of different genes that gave rise to the same physiological interaction. Comparisons on a gene by gene basis may illustrate few common threads, whereas at a pathway level, a trend of perturbation in the expression of genes belonging to the same ontological classes can be observed.

MLG was supported by an NIH Biotechnology Training Grant (GM08347) and a University of Minnesota Graduate School Fellowship.

References

al-Rubeai M, Mills D, Emery AN. 1990. Electron microscopy of hybridoma cells with special regard to monoclonal antibody production. Cytotechnology 4(1):13–28.

Altschul SF, Gish W, Miller W, Myers EW, Lipman DJ. 1990. Basic local alignment search tool. J Mol Biol 215(3):403–410.

Alvarez C, Fujita H, Hubbard A, Sztul E. 1999. ER to Golgi transport: Requirement for p115 at a pre-Golgi VTC stage. J Cell Biol 147(6):1205–1222.

Baik JY, Lee MS, An SR, Yoon SK, Joo EJ, Kim YH, Park HW, Lee GM. 2006. Initial transcriptome and proteome analyses of low culture temperature-induced expression in CHO cells producing erythropoietin. Biotechnol Bioeng 93(2):361–371.

Barnabe N, Butler M. 1994. Effect of temperature on nucleotide pools and monoclonal antibody production in a mouse hybridoma. Biotechnol Bioeng 44(10):1235–1245.

Bartrons R, Carreras J. 1982. Purification and characterization of phosphoglycerate mutase isozymes from pig heart. Biochim Biophys Acta 708(2):167–177.

Beaulieu V, Da Silva N, Pastor-Soler N, Brown CR, Smith PJ, Brown D, Breton S. 2005. Modulation of the actin cytoskeleton via gelsolin regulates vacuolar H+-ATPase recycling. J Biol Chem 280(9):8452–8463.

Blondeau F, Ritter B, Allaire PD, Wasiak S, Girard M, Hussain NK, Angers A, Legendre-Guillemin V, Roy L, Boismenu D, et al. 2004. Tandem MS analysis of brain clathrin-coated vesicles reveals their critical involvement in synaptic vesicle recycling. Proc Natl Acad Sci USA 101(11):3833–3838.

Bossolasco M, Veillette F, Bertrand R, Mes-Masson AM. 2006. Human TDE1, a TDE1/TMS family member, inhibits apoptosis in vitro and stimulates in vivo tumorigenesis. Oncogene 25(33):4549–4558.

Cherlet M, Marc A. 2000. Stimulation of monoclonal antibody production of hybridoma cells by butyrate: Evaluation of a feeding strategy and characterization of cell behavior. Cytotechnology 32:17–29.

Chong L, van Steensel B, Broccoli D, Erdjument-Bromage H, Hanish J, Tempst P, de Lange T. 1995. A human telomeric protein. Science 270(5242):1663–1667.

Chotigeat W, Watanapokasin Y, Mahler S, Gray PP. 1994. Role of environmental conditions on the expression levels, glycoform pattern and levels of sialyltransferase for hFSH produced by recombinant CHO cells. Cytotechnology 15(1–3):217–221.

Chun BH, Park SY, Chung N, Bang WG. 2003. Enhanced production of recombinant B-domain deleted factor VIII from Chinese hamster ovary cells by propionic and butyric acids. Biotechnol Lett 25(4):315–319.

de Leon Gatti M, Wlaschin K, Nissom PM, Yap M, Hu W-S. 2007. Comparative transcriptional analysis of mouse hybridoma and recombinant Chinese hamster ovary cells undergoing butyrate treatment. J Biosci Bioeng 103(1):82–91.

Dinnis DM, Stansfield SH, Schlatter S, Smales CM, Alete D, Birch JR, Racher AJ, Marshall CT, Nielsen LK, James DC. 2006. Functional proteomic analysis of GS-NS0 murine myeloma cell lines with varying recombinant monoclonal antibody production rate. Biotechnol Bioeng 94(5):830–841.

Dorner AJ, Wasley LC, Kaufman RJ. 1989. Increased synthesis of secreted proteins induces expression of glucose-regulated proteins in butyrate-treated Chinese hamster ovary cells. J Biol Chem 264(34):20602–20607.

Dulic V, Lees E, Reed SI. 1992. Association of human cyclin E with a periodic G1-S phase protein kinase. Science 257(5078):1958–1961.

Ekholm SV, Reed SI. 2000. Regulation of G(1) cyclin-dependent kinases in the mammalian cell cycle. Curr Opin Cell Biol 12(6):676–684.

Exton JH. 1997. New developments in phospholipase D. J Biol Chem 272(25):15579–15582.

Farges-Haddani B, Tessier B, Chenu S, Chevalot I, Harscoat C, Marc I, Goergen JL, Marc A. 2006. Peptide fractions of rapeseed hydrolysates as an alternative to animal proteins in CHO cell culture media. Process Biochem 41(11):2297–2304.

Fogolin MB, Wagner R, Etcheverrigaray M, Kratje R. 2004. Impact of temperature reduction and expression of yeast pyruvate carboxylase on hGM-CSF-producing CHO cells. J Biotechnol 109(1–2):179–191.

Gorman CM, Howard BH, Reeves R. 1983. Expression of recombinant plasmids in mammalian cells is enhanced by sodium butyrate. Nucleic Acids Res 11(21):7631–7648.

Harper JW, Adami GR, Wei N, Keyomarsi K, Elledge SJ. 1993. The p21 Cdk-interacting protein Cip1 is a potent inhibitor of G1 cyclin-dependent kinases. Cell 75(4):805–816.

Hayduk EJ, Lee KH. 2005. Cytochalasin D can improve heterologous protein productivity in adherent Chinese hamster ovary cells. Biotechnol Bioeng 90(3):354–364.

Hendrick V, Winnepenninckx P, Abdelkafi C, Vandeputte O, Cherlet M, Marique T, Renemann G, Loa A, Kretzmer G, Werenne J. 2001. Increased productivity of recombinant tissular plasminogen activator (t-Pa) by butyrate and shift of temperature: A cell cycle phases analysis. Cytotechnology 36:71–83.

Hinds PW, Mittnacht S, Dulic V, Arnold A, Reed SI, Weinberg RA. 1992. Regulation of retinoblastoma protein functions by ectopic expression of human cyclins. Cell 70(6):993–1006.

Kim NS, Lee GM. 2000. Overexpression of bcl-2 inhibits sodium butyrate-induced apoptosis in Chinese hamster ovary cells resulting in enhanced humanized antibody production. Biotechnol Bioeng 71(3):184–193.

Korke R, Gatti Mde L, Lau AL, Lim JW, Seow TK, Chung MC, Hu WS. 2004. Large scale gene expression profiling of metabolic shift of mammalian cells in culture. J Biotechnol 107(1):1–17.

Koshikawa N, Maejima C, Miyazaki K, Nakagawara A, Takenaga K. 2006. Hypoxia selects for high-metastatic Lewis lung carcinoma cells over-expressing Mcl-1 and exhibiting reduced apoptotic potential in solid tumors. Oncogene 25(6):917–928.

Larance M, Ramm G, Stockli J, van Dam EM, Winata S, Wasinger V, Simpson F, Graham M, Junutula JR, Guilhaus M, et al. 2005. Characterization of the role of the Rab GTPase-activating protein AS160 in insulin-regulated GLUT4 trafficking. J Biol Chem 280(45):37803–37813.

Lees E, Faha B, Dulic V, Reed SI, Harlow E. 1992. Cyclin E/cdk2 and cyclin A/cdk2 kinases associate with p107 and E2F in a temporally distinct manner. Genes Dev 6(10):1874–1885.

Leschelle X, Delpal S, Goubern M, Blottiere HM, Blachier F. 2000. Butyrate metabolism upstream and downstream acetyl-CoA synthesis and growth control of human colon carcinoma cells. Eur J Biochem 267(21):6435–6442.

Lozupone F, Lugini L, Matarrese P, Luciani F, Federici C, Iessi E, Margutti P, Stassi G, Malorni W, Fais S. 2004. Identification and relevance of the CD95-binding domain in the N-terminal region of ezrin. J Biol Chem 279(10):9199–9207.

Ma K, Vattem KM, Wek RC. 2002. Dimerization and release of molecular chaperone inhibition facilitate activation of eukaryotic initiation factor-2 kinase in response to endoplasmic reticulum stress. J Biol Chem 277(21):18728–18735.

Mangeat P, Roy C, Martin M. 1999. ERM proteins in cell adhesion and membrane dynamics. Trends Cell Biol 9(5):187–192.

Mazur X, Fussenegger M, Renner WA, Bailey JE. 1998. Higher productivity of growth-arrested Chinese hamster ovary cells expressing the cyclin-dependent kinase inhibitor p27. Biotechnol Prog 14(5):705–713.

Mimura Y, Lund J, Church S, Dong S, Li J, Goodall M, Jefferis R. 2001. Butyrate increases production of human chimeric IgG in CHO-K1 cells whilst maintaining function and glycoform profile. J Immunol Methods 247(1–2):205–216.

Morris JA, Dorner AJ, Edwards CA, Hendershot LM, Kaufman RJ. 1997. Immunoglobulin binding protein (BiP) function is required to protect cells from endoplasmic reticulum stress but is not required for the secretion of selective proteins. J Biol Chem 272(7):4327–4334.

Oh SKW, Vig P, Chua F, Teo WK, Yap MGS. 1993. Substantial overproduction of antibodies by applying osmotic pressure and sodium butyrate. Biotechnol Bioeng 42:601–610.

Ohashi M, Jan de Vries K, Frank R, Snoek G, Bankaitis V, Wirtz K, Huttner WB. 1995. A role for phosphatidylinositol transfer protein in secretory vesicle formation. Nature 377(6549):544–547.

Palermo DP, DeGraaf ME, Marotti KR, Rehberg E, Post LE. 1991. Production of analytical quantities of recombinant proteins in Chinese hamster ovary cells using sodium butyrate to elevate gene expression. J Biotechnol 19(1):35–47.

Panaretakis T, Pokrovskaja K, Shoshan MC, Grander D. 2003. Interferon-alpha-induced apoptosis in U266 cells is associated with activation of the proapoptotic Bcl-2 family members Bak and Bax. Oncogene 22(29):4543–4556.

Pelle R, Murphy NB. 1993. Northern hybridization: rapid and simple electrophoretic conditions. Nucleic Acids Res 21(11):2783–2784.

Pines J. 1995. Cyclins and cyclin-dependent kinases: A biochemical view. Biochem J 308(Pt 3):697–711.

Riggs MG, Whittaker RG, Neumann JR, Ingram VM. 1977. n-Butyrate causes histone modification in HeLa and Friend erythroleukaemia cells. Nature 268(5619):462–464.

Romijn EP, Christis C, Wieffer M, Gouw JW, Fullaondo A, van der Sluijs P, Braakman I, Heck AJ. 2005. Expression clustering reveals detailed co-expression patterns of functionally related proteins during B cell differentiation: A proteomic study using a combination of one-dimensional gel electrophoresis, LC-MS/MS, and stable isotope labeling by amino acids in cell culture (SILAC). Mol Cell Proteomics 4(9):1297–1310.

Santoni V, Molloy M, Rabilloud T. 2000. Membrane proteins and proteomics: Un amour impossible? Electrophoresis 21(6):1054– 1070.

Seth G, Philp RJ, Denoya CD, McGrath K, Stutzman-Engwall KJ, Yap M, Hu WS. 2005. Large-scale gene expression analysis of cholesterol dependence in NS0 cells. Biotechnol Bioeng 90(5):552– 567.

Seth G, Philp RJ, Lau A, Jiun KY, Yap M, Hu WS. 2006. Molecular portrait of high productivity in recombinant NS0 cells. Biotechnol Bioeng 97(4):933–951.

Shaffer AL, Shapiro-Shelef M, Iwakoshi NN, Lee AH, Qian SB, Zhao H, Yu X, Yang L, Tan BK, Rosenwald A, et al. 2004. XBP1, downstream of Blimp-1, expands the secretory apparatus and other organelles, and increases protein synthesis in plasma cell differentiation. Immunity 21(1):81–93.

Shen D, Sharfstein ST. 2006. Genome-wide analysis of the transcriptional response of murine hybridomas to osmotic shock. Biotechnol Bioeng 93(1):132–145.

Starr DA, Williams BC, Li Z, Etemad-Moghadam B, Dawe RK, Goldberg ML. 1997. Conservation of the centromere/kinetochore protein ZW10. J Cell Biol 138(6):1289–1301.

Susin SA, Daugas E, Ravagnan L, Samejima K, Zamzami N, Loeffler M, Costantini P, Ferri KF, Irinopoulou T, Prevost MC, et al. 2000. Two distinct pathways leading to nuclear apoptosis. J Exp Med 192(4):571–580.

van Anken E, Romijn EP, Maggioni C, Mezghrani A, Sitia R, Braakman I, Heck AJ. 2003. Sequential waves of functionally related proteins are expressed when B cells prepare for antibody secretion. Immunity 18(2):243–253.

Van Dyk DD, Misztal DR, Wilkins MR, Mackintosh JA, Poljak A, Varnai JC, Teber E, Walsh BJ, Gray PP. 2003. Identification of cellular changes associated with increased production of human growth hormone in a recombinant Chinese hamster ovary cell line. Proteomics 3(2):147–156.

Varma D, Dujardin DL, Stehman SA, Vallee RB. 2006. Role of the kinetochore/cell cycle checkpoint protein ZW10 in interphase cytoplasmic dynein function. J Cell Biol 172(5):655–662.

Wang MD, Yang M, Huzel N, Butler M. 2002. Erythropoietin production from CHO cells grown by continuous culture in a fluidized-bed bioreactor. Biotechnol Bioeng 77(2):194–203.

Wlaschin KF, Nissom PM, Gatti Mde L, Ong PF, Arleen S, Tan KS, Rink A, Cham B, Wong K, Yap M, et al. 2005. EST sequencing for genediscovery in Chinese hamster ovary cells. Biotechnol Bioeng 91(5):592–606.

Woo M, Hakem A, Elia AJ, Hakem R, Duncan GS, Patterson BJ, Mak TW. 1999. In vivo evidence that caspase-3 is required for Fas-mediated apoptosis of hepatocytes. J Immunol 163(9):4909–4916.

Wurm FM. 2004. Production of recombinant protein therapeutics in cultivated mammalian cells. Nat Biotechnol 22(11):1393–1398.

Yamamoto K, Fujii R, Toyofuku Y, Saito T, Koseki H, Hsu VW, Aoe T. 2001. The KDEL receptor mediates a retrieval mechanism that contributes to quality control at the endoplasmic reticulum. EMBO J 20(12):3082–3091.

Yoon SK, Kim SH, Lee GM. 2003. Effect of low culture temperature on specific productivity and transcription level of anti-4-1BB antibody in recombinant Chinese hamster ovary cells. Biotechnol Prog 19(4):1383–1386.

Zhang HM, Yanagawa B, Cheung P, Luo H, Yuan J, Chau D, Wang A, Bohunek L, Wilson JE, McManus BM, et al. 2002. Nip21 gene expression reduces coxsackievirus B3 replication by promoting apoptotic cell death via a mitochondria-dependent pathway. Circ Res 90(12):1251–1258.

Zhou WC, Rehm J, Hu WS. 1995. High viable cell concentration fed-batch cultures of hybridoma cells through online nutrient feeding. Biotechnol Bioeng 46:579–587.